Constraints on dark matter from astrophysical observations of the Milky Way's dwarf spheroidal galaxies

Miho N. Ishigaki (Tohoku University, Astronomical Institute)

On behalf of

S. Horigome (U. Tokyo/Kavli IPMU)

K. Hayashi (ICRR)

S. Matsumoto (Kavli IPMU)

M. Ibe (Kavli IPMU)

M. Sugai (Kavli IPMU)

K. Ichikawa (former grad. student of U. Tokyo)

See Hayashi et al. 2016, Ichikawa et al. 2017, Ichikawa et al. 2018

43th John Hopkins Workshop

Kavli IPMU, June 5th 2019

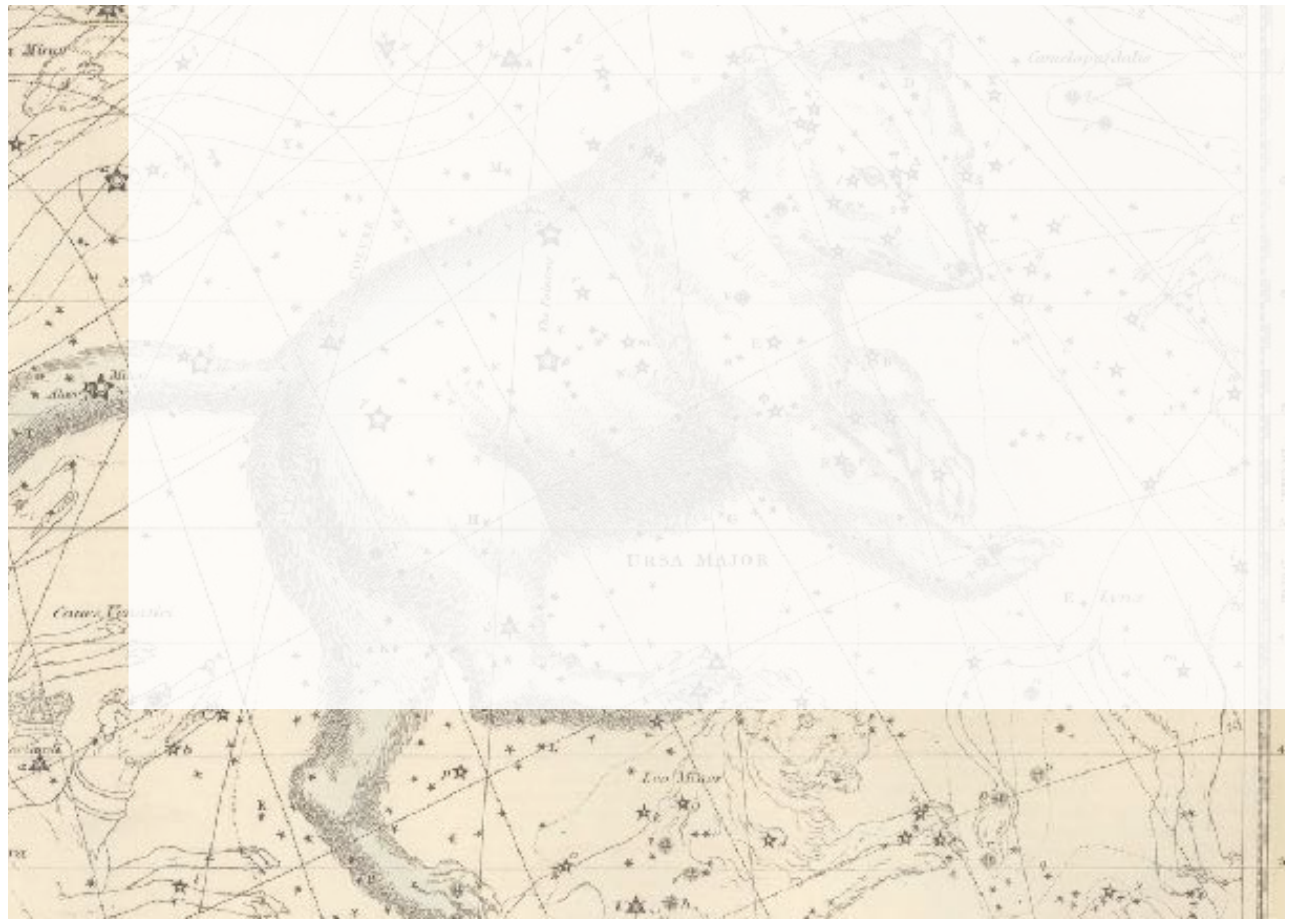

Our team is strong

Koji Ichikawa
Former PhD student of U. Tokyo

Masahiro Ibe
ICRR

Shigeki Matsumoto
IPMU

Shunichi Horigome
IPMU, U. Tokyo Grad student

Particle physics

Astrophysics

Hajime Sugai
IPMU

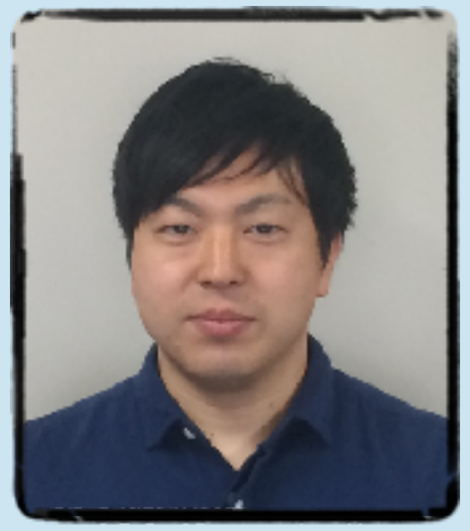

Kohei Hayashi
ICRR

Miho N. Ishigaki
Tohoku U.

Outline

- Dark matter content in dwarf spheroidal galaxies (dSphs) based on stellar spectroscopic observations
- Our study: the effect of contaminating stars on the estimation of dark matter profiles in dwarf spheroidal galaxies
- Future prospects with new observational facilities

Quantification of all possible sources of uncertainties in stellar spectroscopic measurements is essential for the robust estimates of expected γ-ray flux from dark matter annihilation

Dwarf spheroidal satellite galaxies (dSphs) around the Milky Way

Drlica-Wagner et al. arXiv:1508.03622

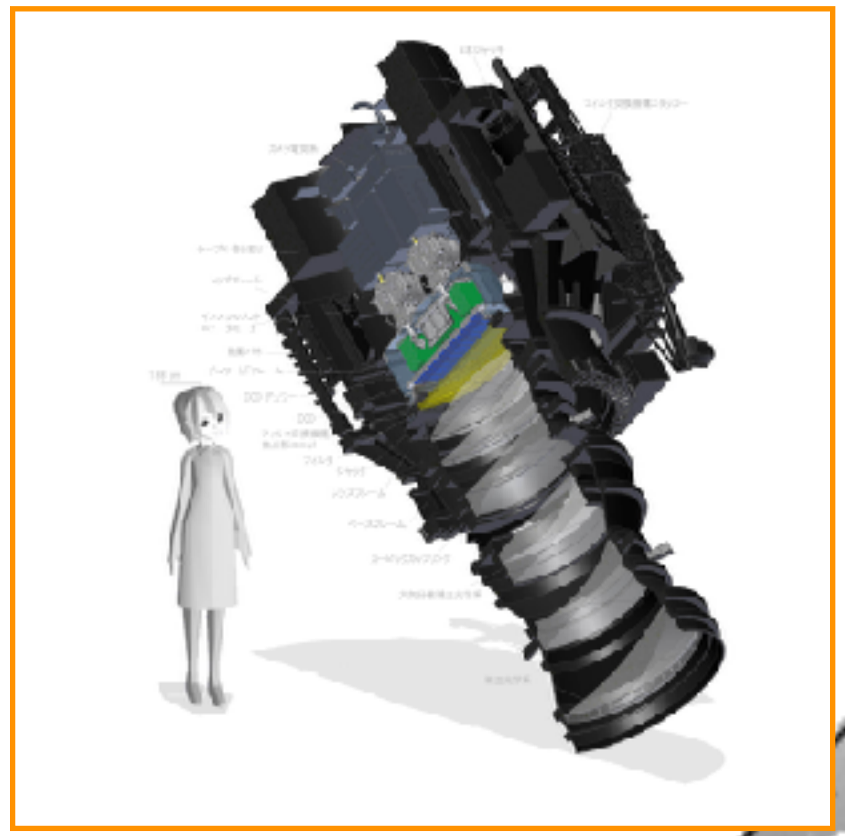

Hyper Suprime Cam on the Subaru Telescope

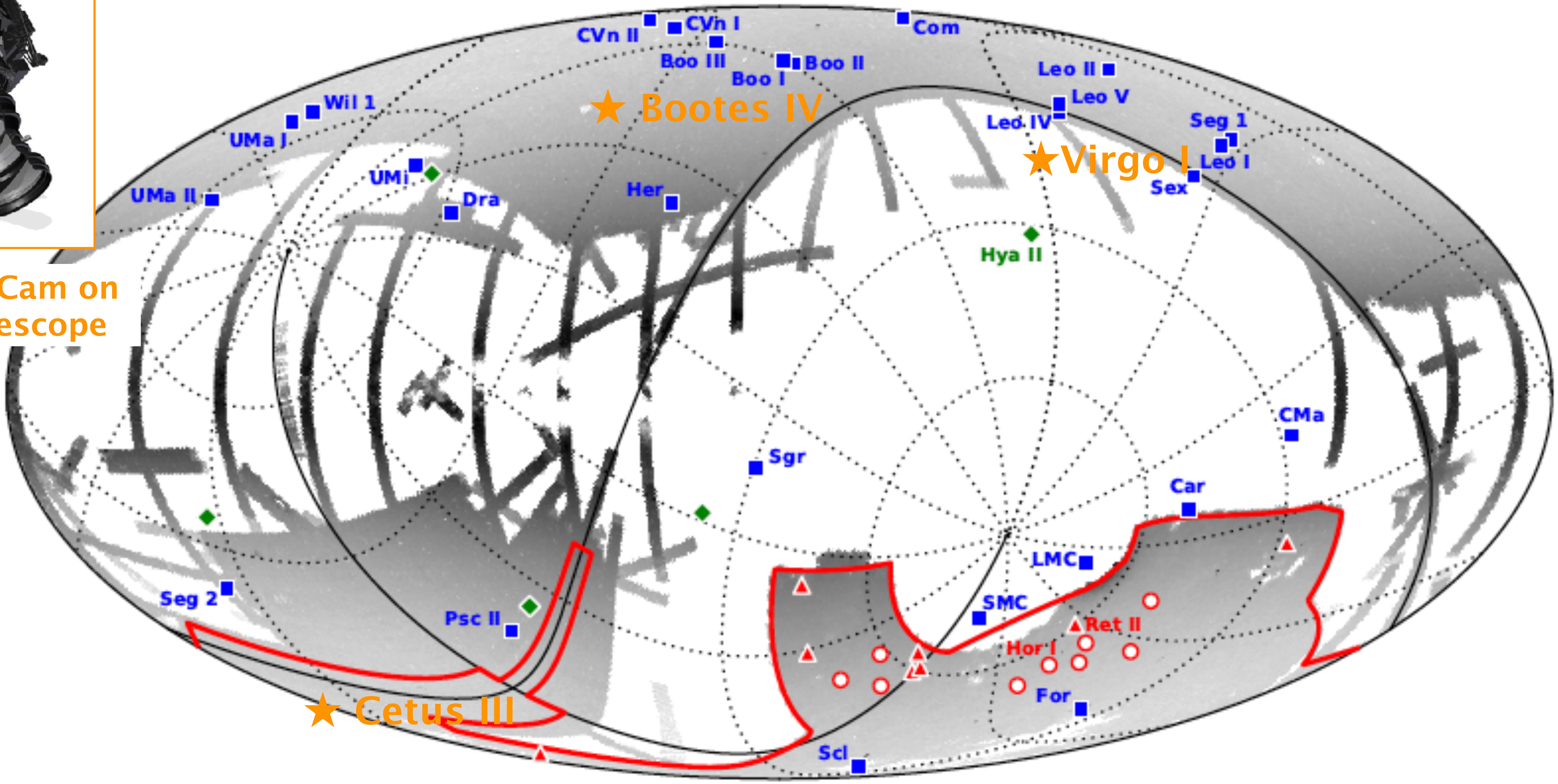

Searches for γ-rays associated with dark matter annihilation

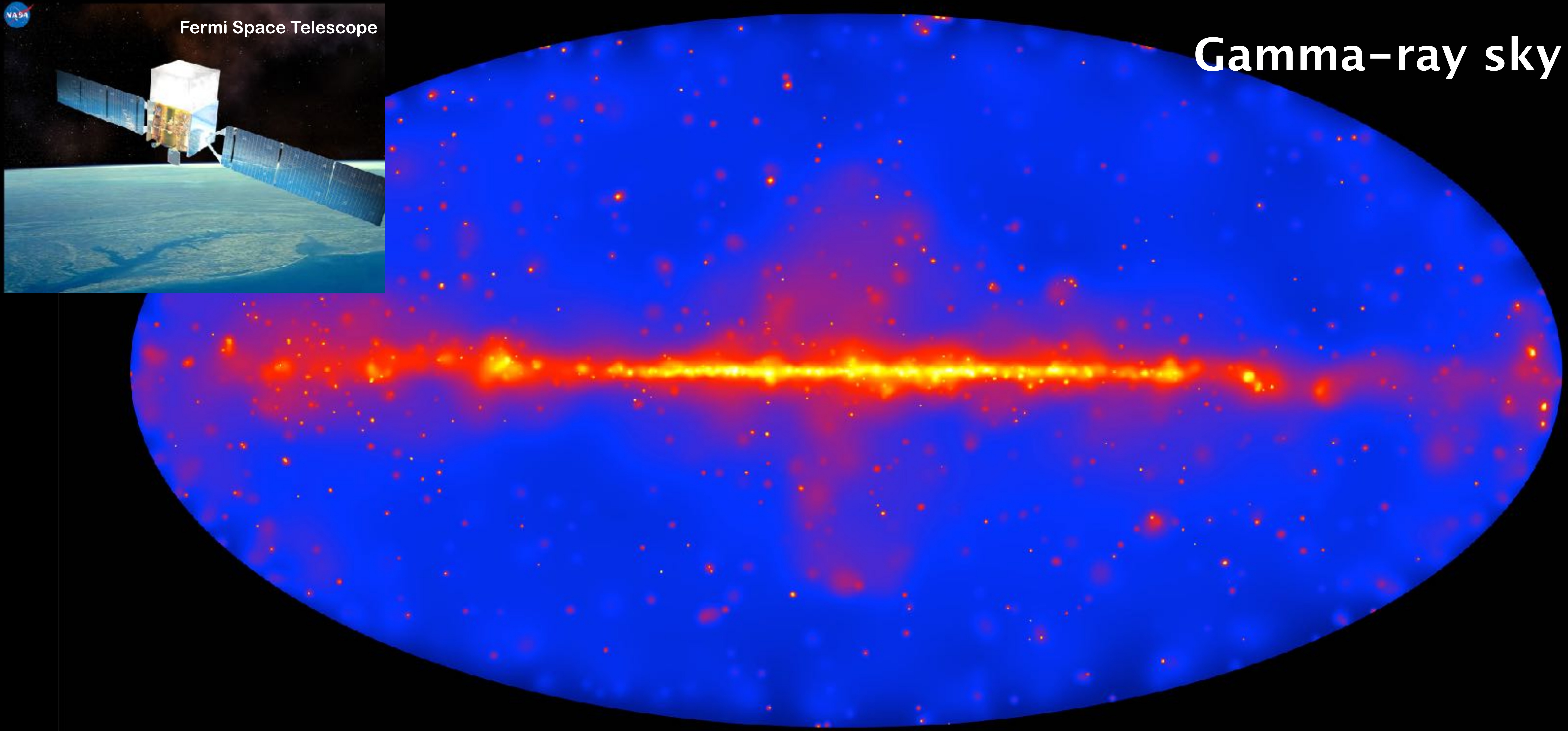

Why dSphs?

- Dark matter dominated: dark matter mass > 10–1000 times stellar mass
- Low astrophysical back ground: c.f. the Galactic center contains pulsars
- Nearby: 30–100 kpc

However…various sources of uncertainties in the dark matter profile estimates from stellar kinematic measurements

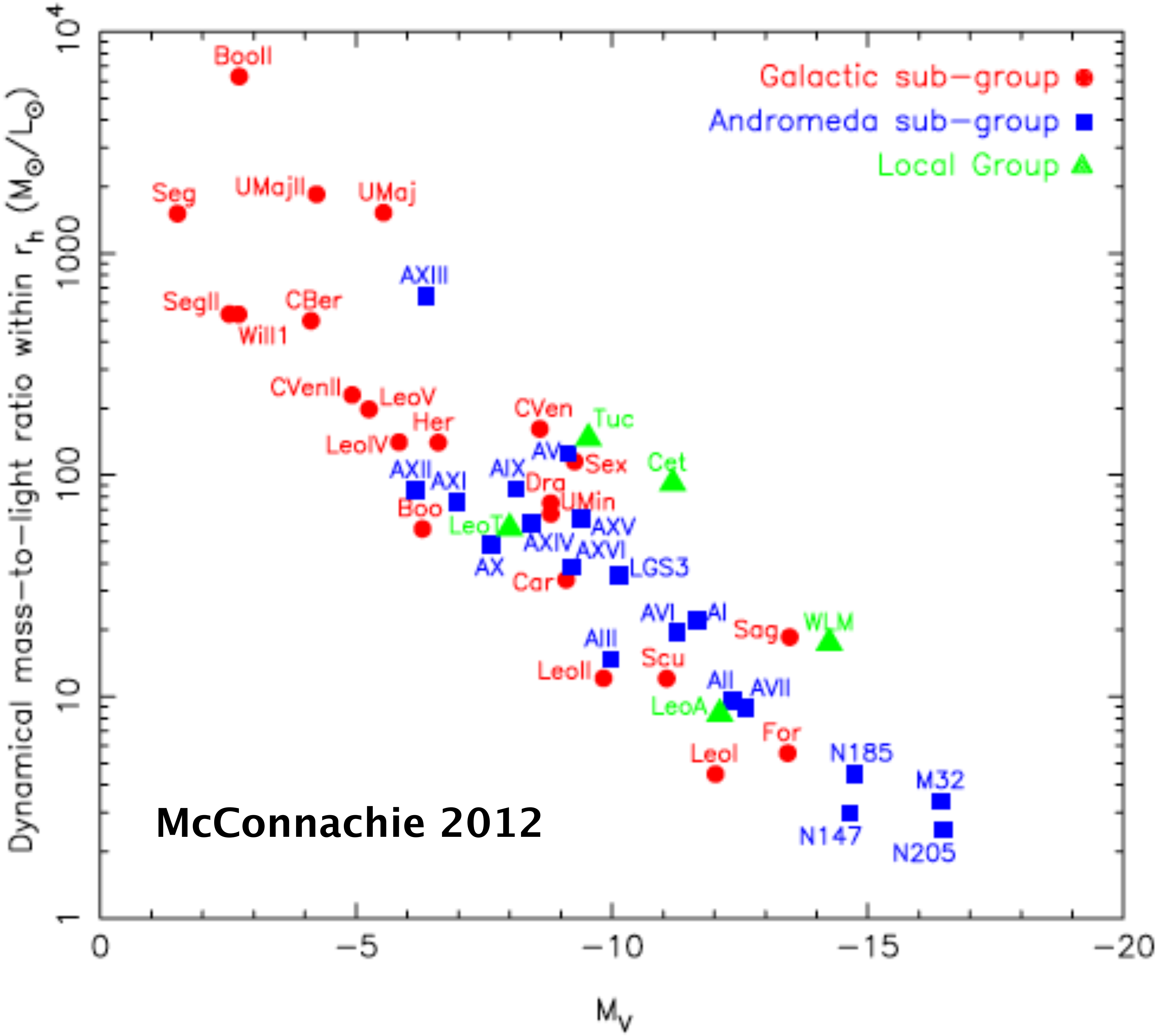

Annihilation gamma-ray flux

- Dark matter particle mass
- Averaged annihilation cross-section $\langle\sigma v\rangle$
- Energy spectrum of annihilation products
- J-factor

$$J(\Delta\Omega) = \int_{\Delta\Omega} d\Omega \int \rho_{\mathrm{DM}}^2(l, \Omega) dl$$

A systematic uncertainty in ρ_{DM}

➡ a few orders of magnitudes variation in the J-factor estimates

Estimates of DM distribution

- Dark matter density distribution

$$\rho_{\rm DM}(r) = \rho_s (r/r_s)^{-\gamma}(1 + (r/r_s)^{\alpha})^{-(\beta-\gamma)/\alpha}$$

ρ_s : typical density

r_s : scale radius

α, β, γ : shape of the DM density profile

- The density profile is connected to the velocity dispersion through the Jeans equation

$$\frac{1}{\nu_*(r)}\frac{\partial}{\partial r}\nu_*(r)\sigma_r^2(r) + \frac{2\beta_{\rm ani}(r)\sigma_r^2(r)}{r} = -\frac{GM(r)}{r^2} \qquad \beta_{\rm ani} = 1 - \sigma_\theta^2/\sigma_r^2$$

- Line-of-sight velocity dispersion to be compared with observation

$$\sigma_{\rm l.o.s}^2(R) = \frac{2}{\Sigma_*(R)}\int_R^\infty dr \left(1 - \beta_{\rm ani}(r)\frac{R^2}{r^2}\right)\frac{\nu_*(r)\sigma_r^2(r)}{\sqrt{1 - R^2/r^2}} \Longleftrightarrow \text{Observed velocity dispersion profile}$$

Spectroscopic observation

The Color-magnitude diagram for Segue 2

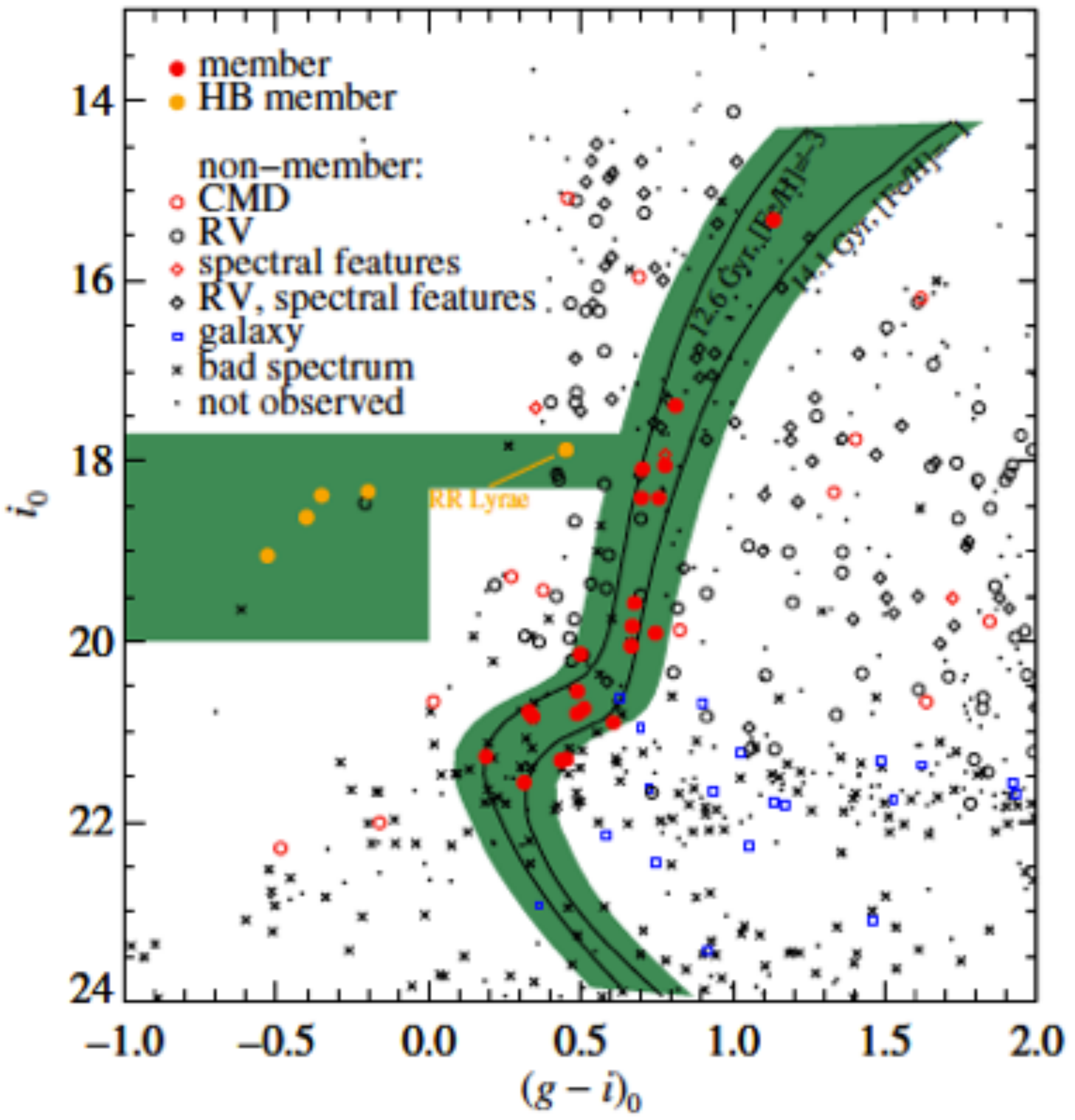

The stellar positions overlaid by slit masks of Keck/DEIMOS

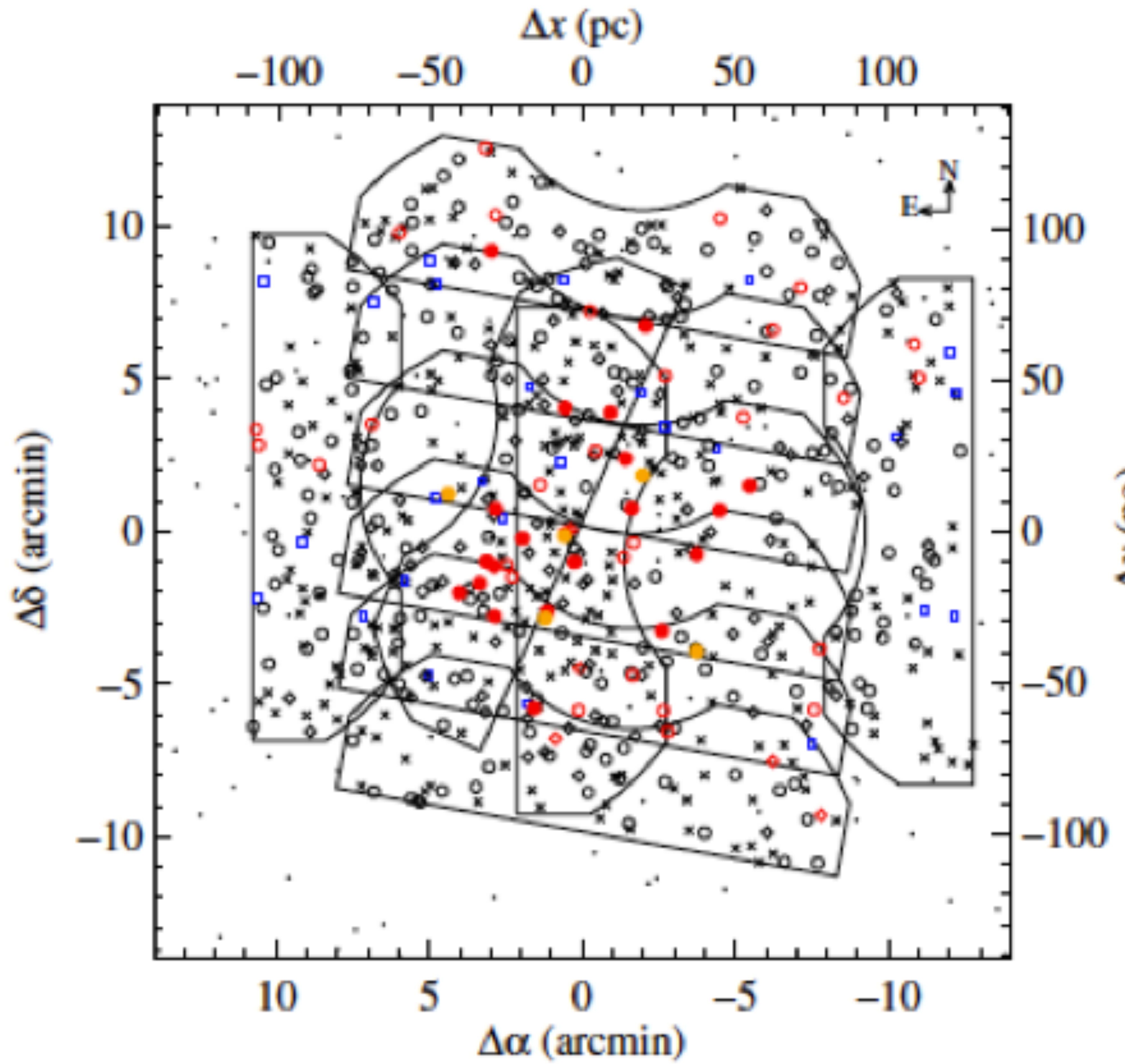

Kirby et al. 2013

Line-of-sight velocity measurements

Kirby et al. 2013

Absorption lines of singly ionized Calcium

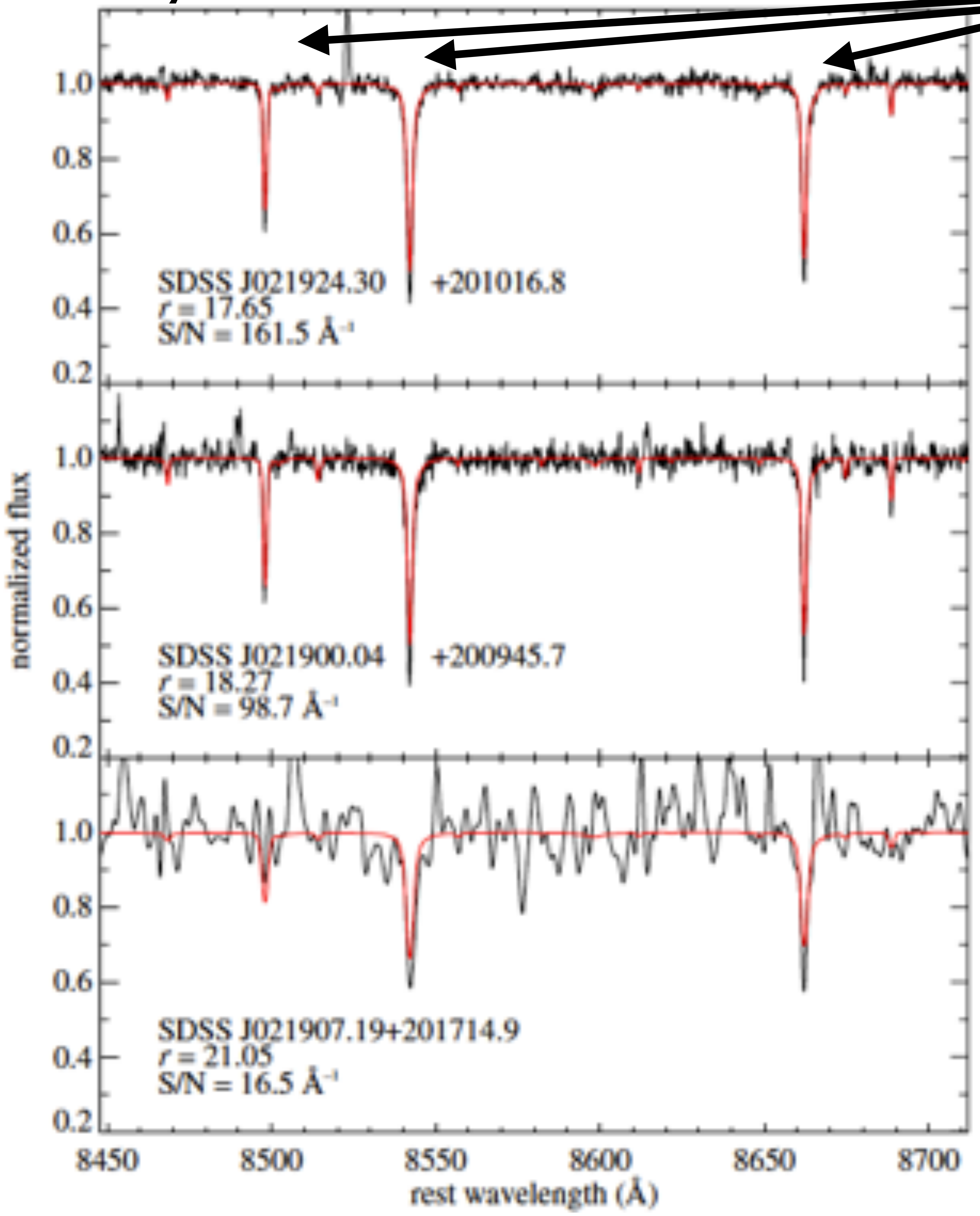

- Wavelength shifts with respect to the rest frame
  ➡ line-of-sight velocity
- Strength of the absorption lines
  ➡ chemical composition

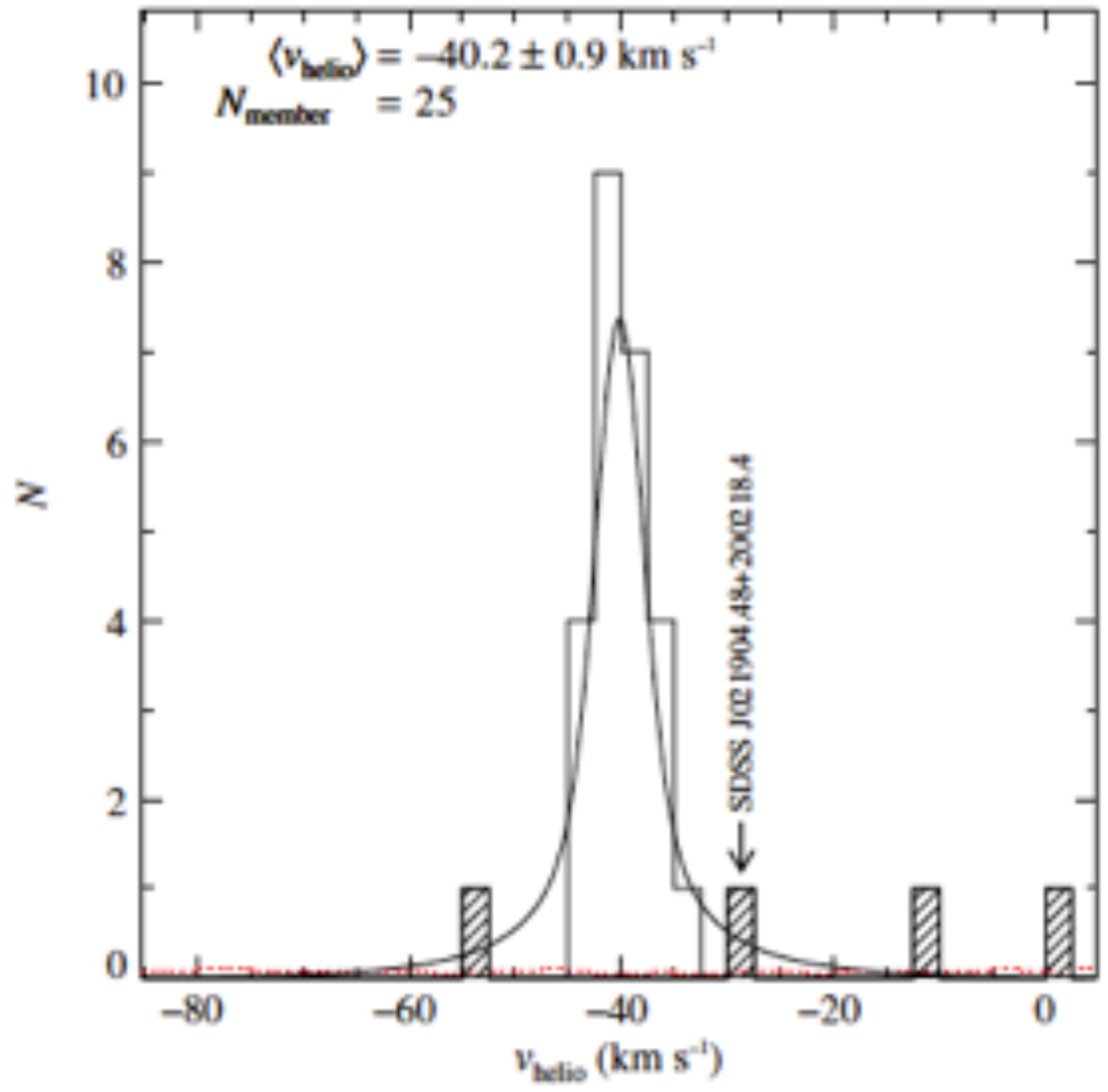

Velocity dispersion profile

Walker et al. 2007

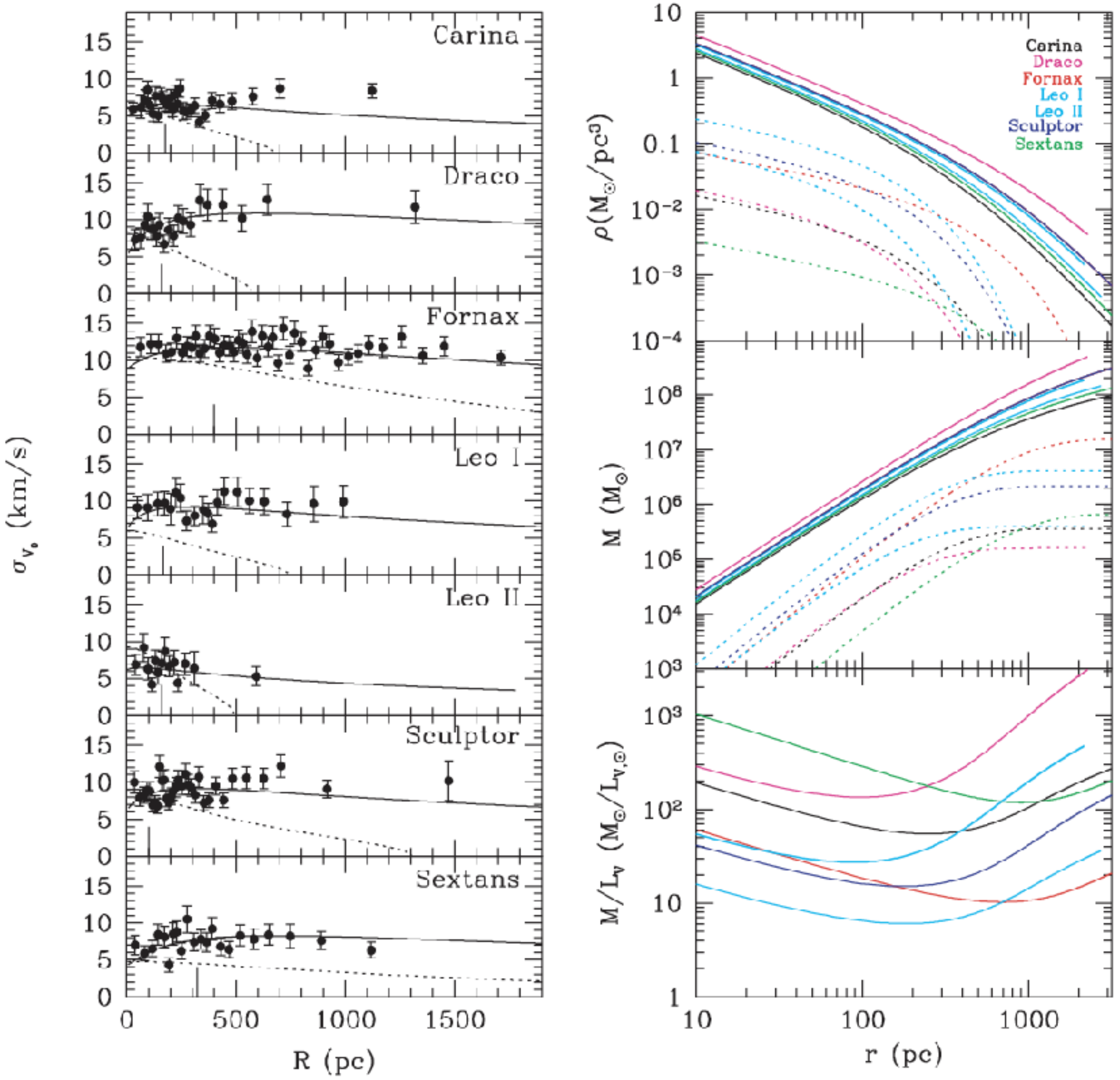

Walker et al. 2009

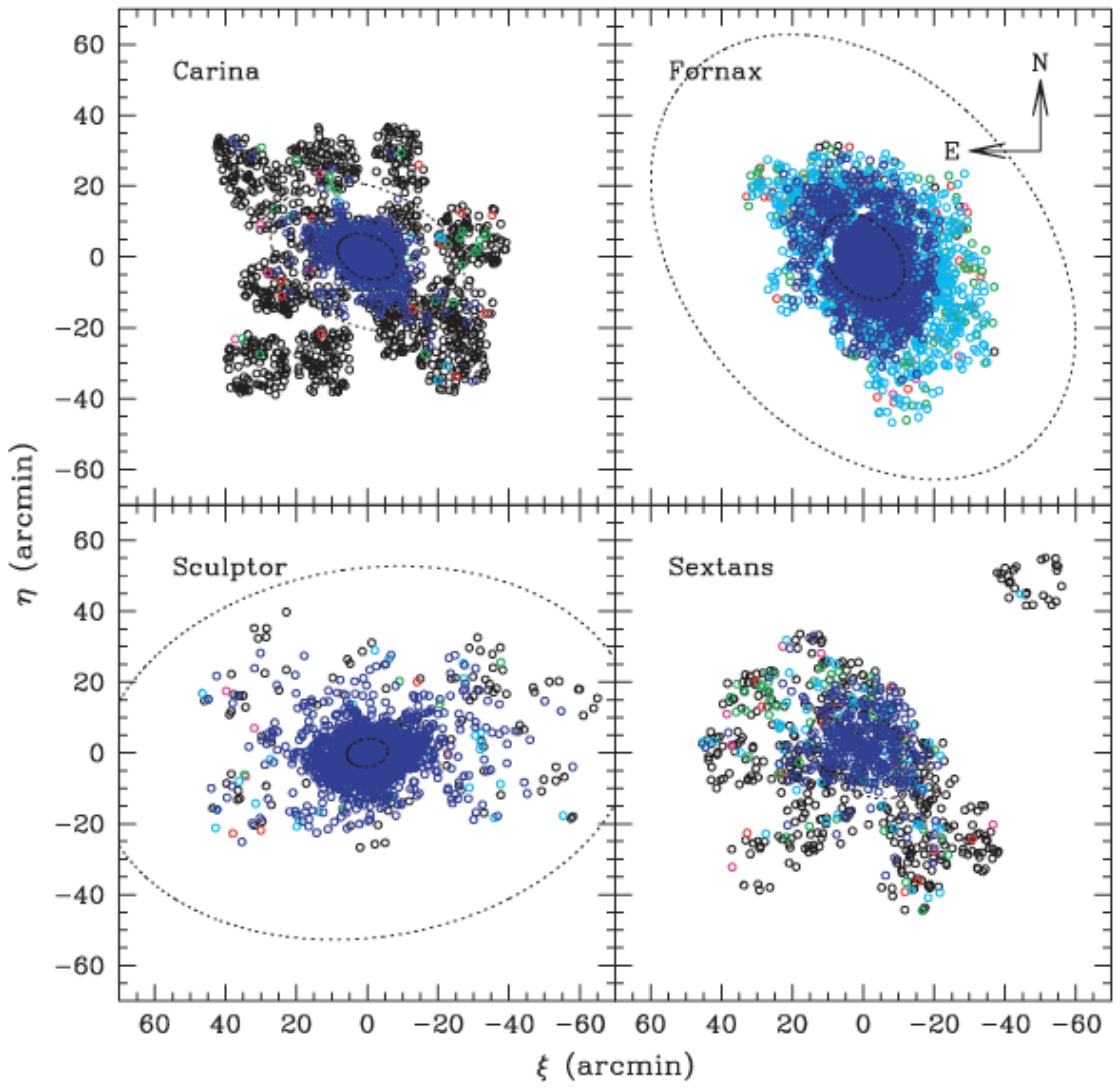

- 200–2000 stars in 7 luminous (classical) dSphs
- Outer regions up to the tidal radii are not fully sampled

Assumptions

- Dynamic equilibrium
- Spherical symmetry
- Constant velocity anisotropy at all radii $\beta_{\rm ani} = \text{constant}$
- Orbital motions of the unresolved binary stars are negligible compared to the velocity dispersion of the system
- All of the stars are the genuine members of the galaxy

Validity of dynamic equilibrium

Proper motion estimates for the Sculptor dSph (Iorio et al. 2019)

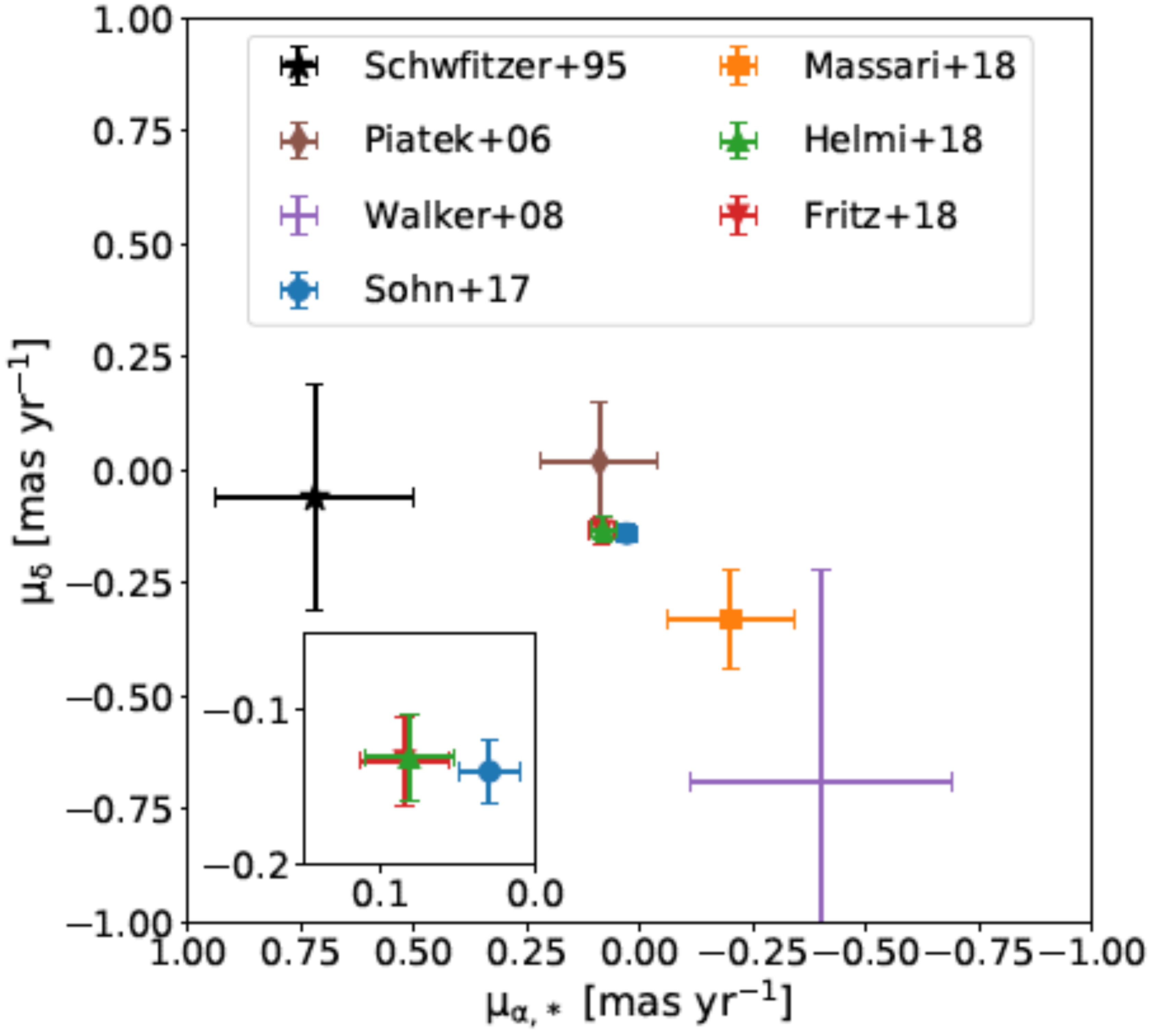

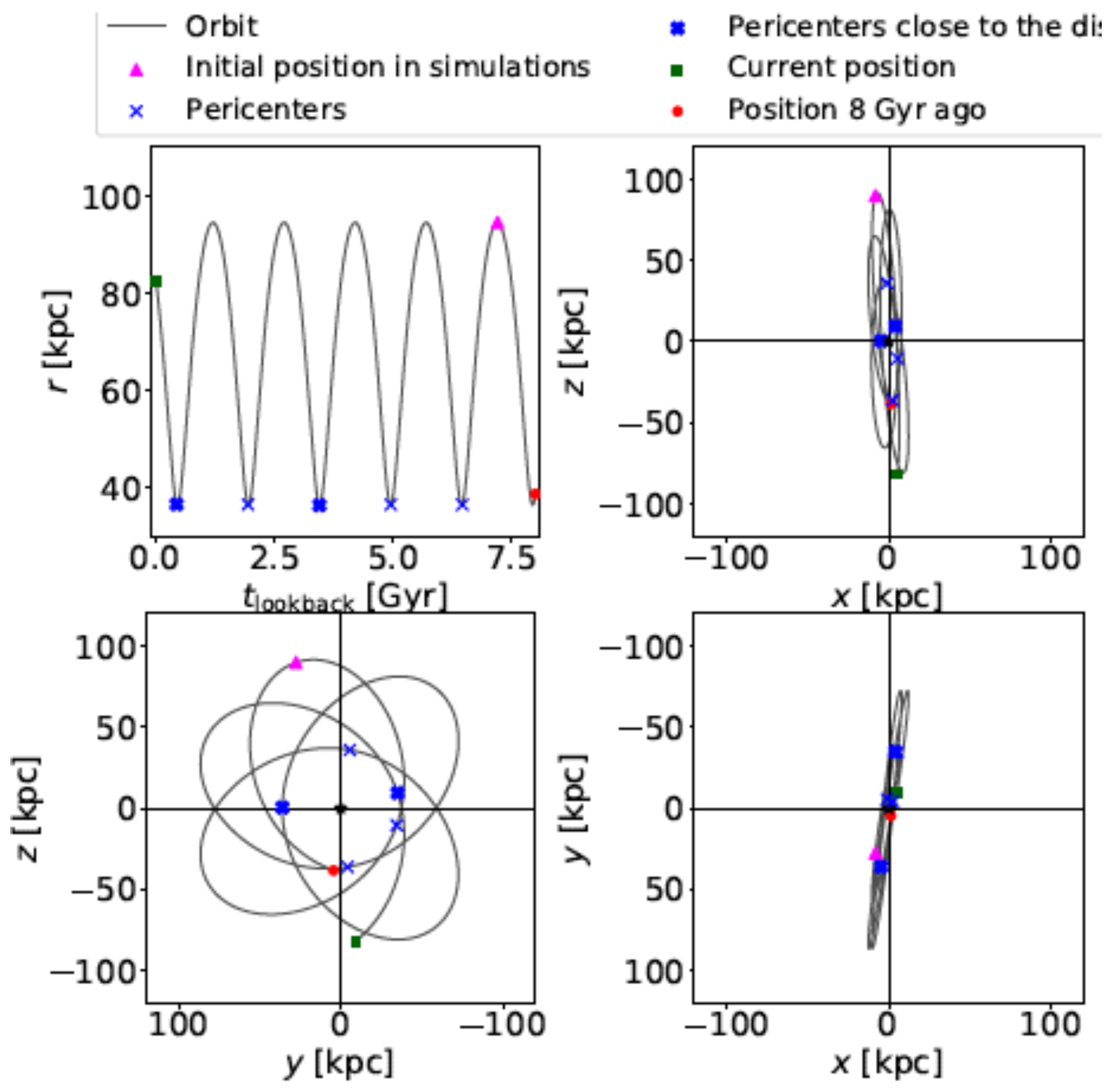

The Sculptor is not affected by the tidal field of the Milky Way and is close to dynamic equilibrium in its own dark matter halo

Spherical symmetry

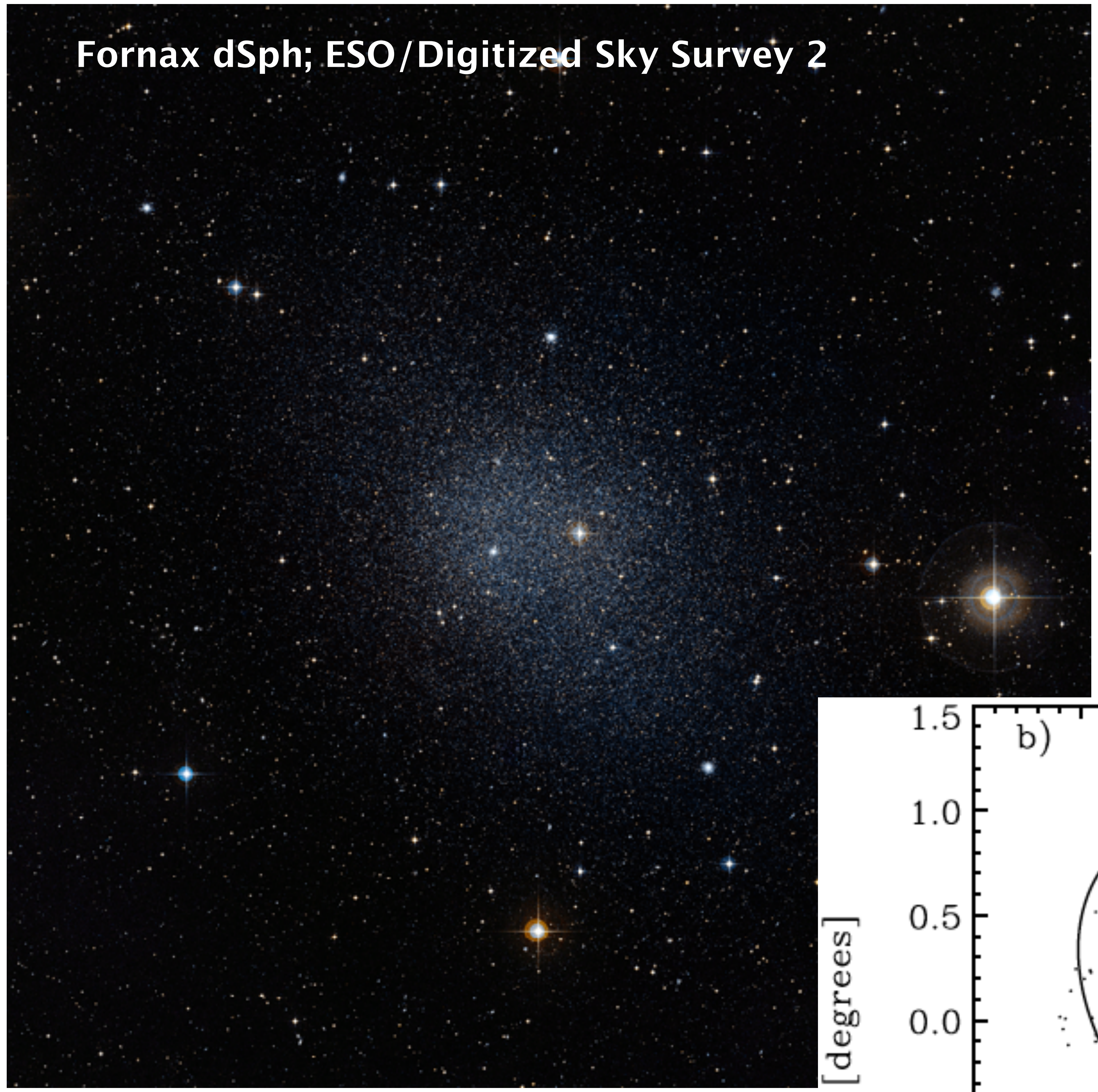

Battaglia et al. 2006

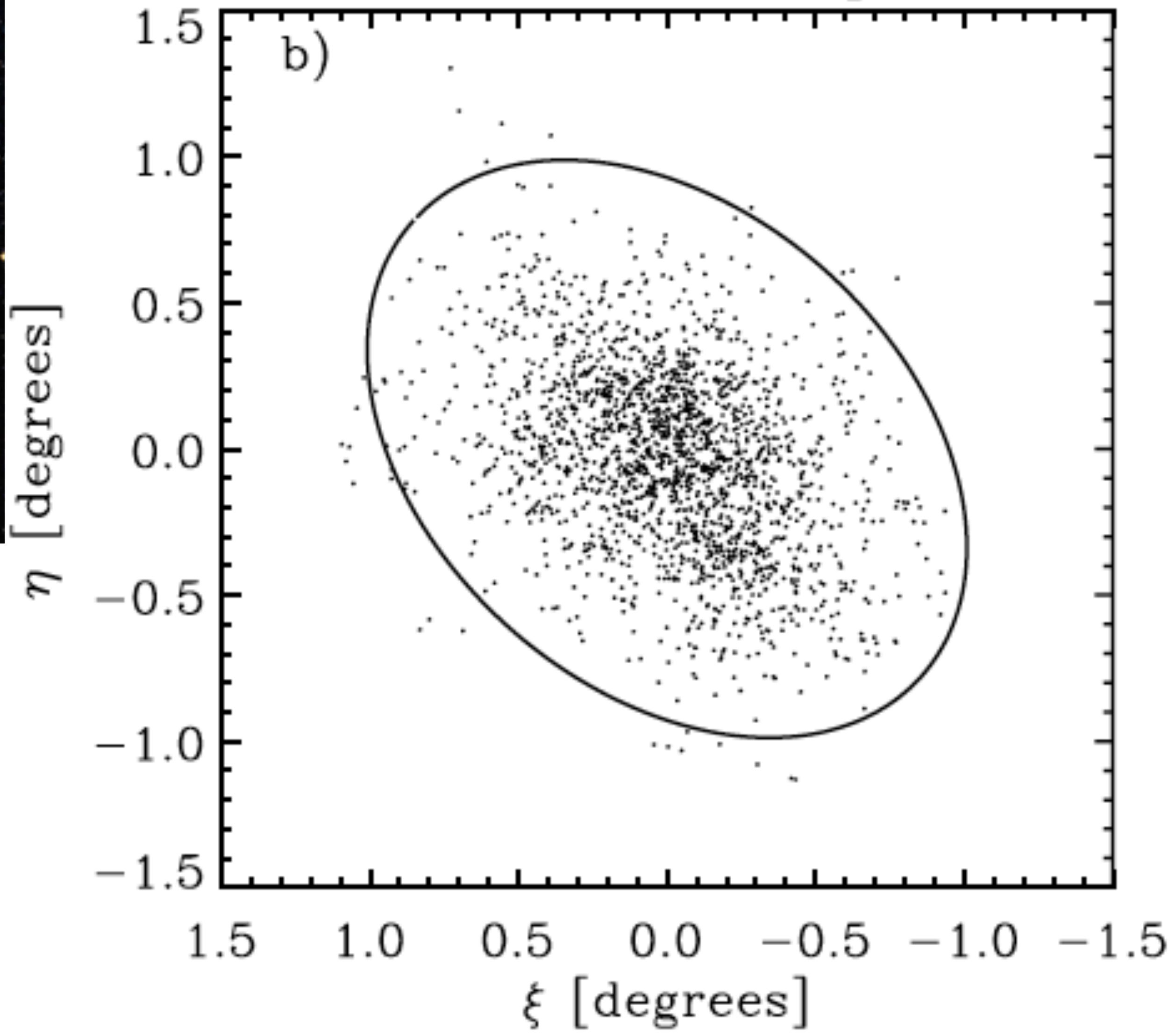

- Projected axial ratio (classical dSphs): 0.65–0.87 (**Hayashi et al. 2016**)

- Up to a few orders of magnitude difference in the J-factor estimates (**Hayashi et al. 2016**, see also Hayashi & Chiba 2012, 2015)

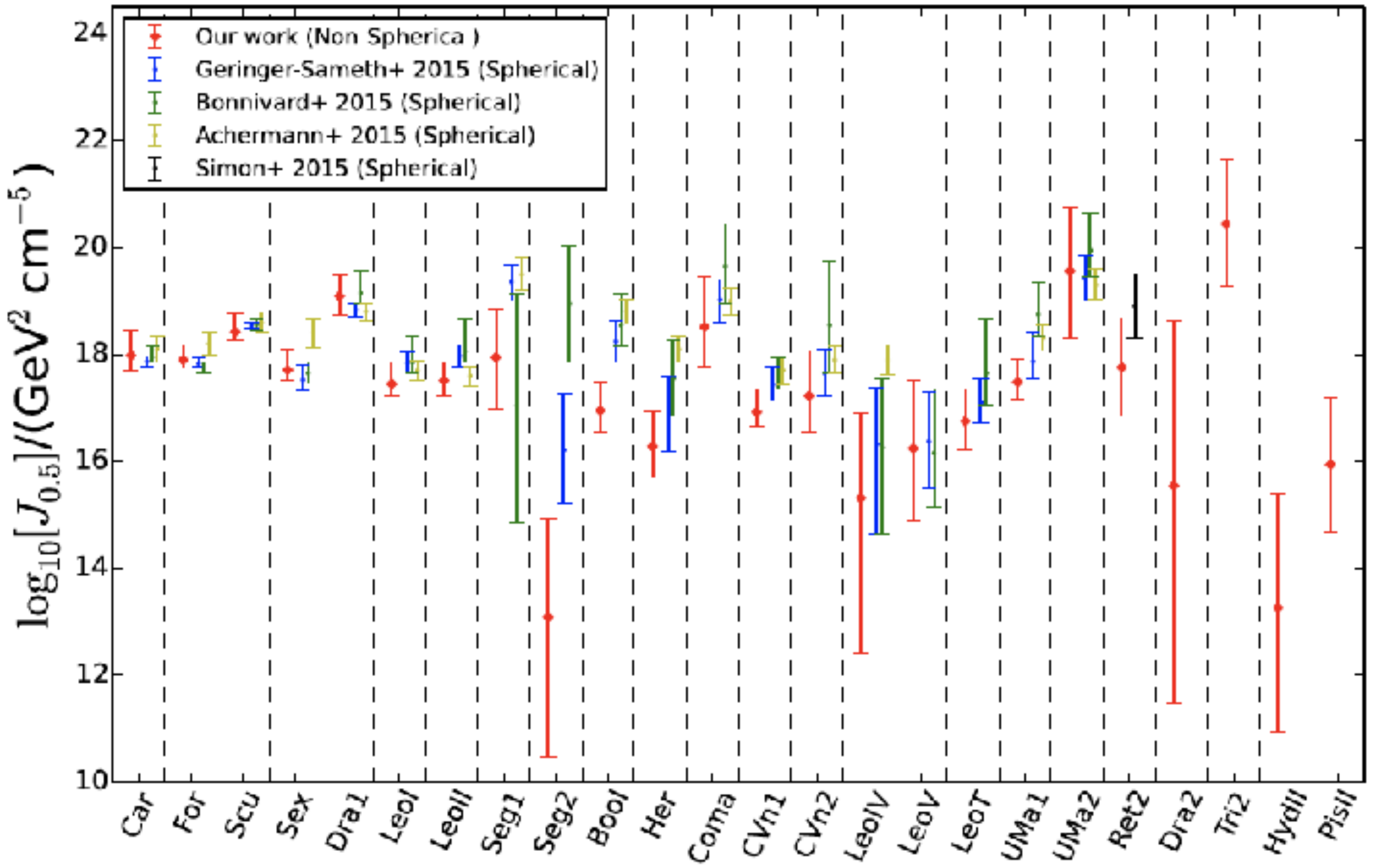

Velocity anisotropy

The first measurement of β_{ani} in a galaxy other than the Milky Way (Masari et al. 2019)

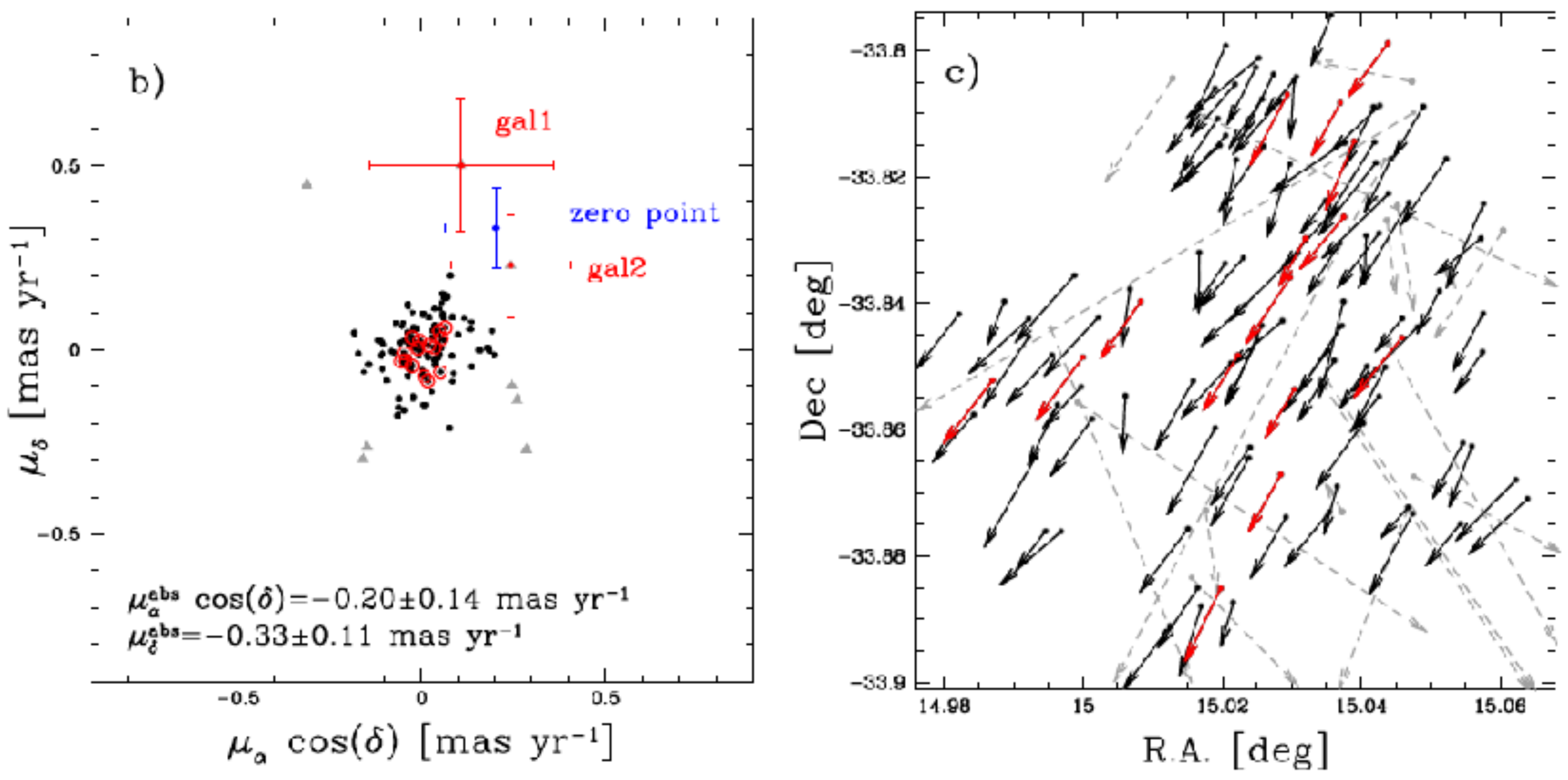

Proper motion of individual stars in the Sculptor dSph

- The baseline of 12.27 years with HST and Gaia
- Distant background galaxies (no proper motion) as a reference

$$\beta_{ani} \sim 0.86^{+0.12}_{-0.83}$$

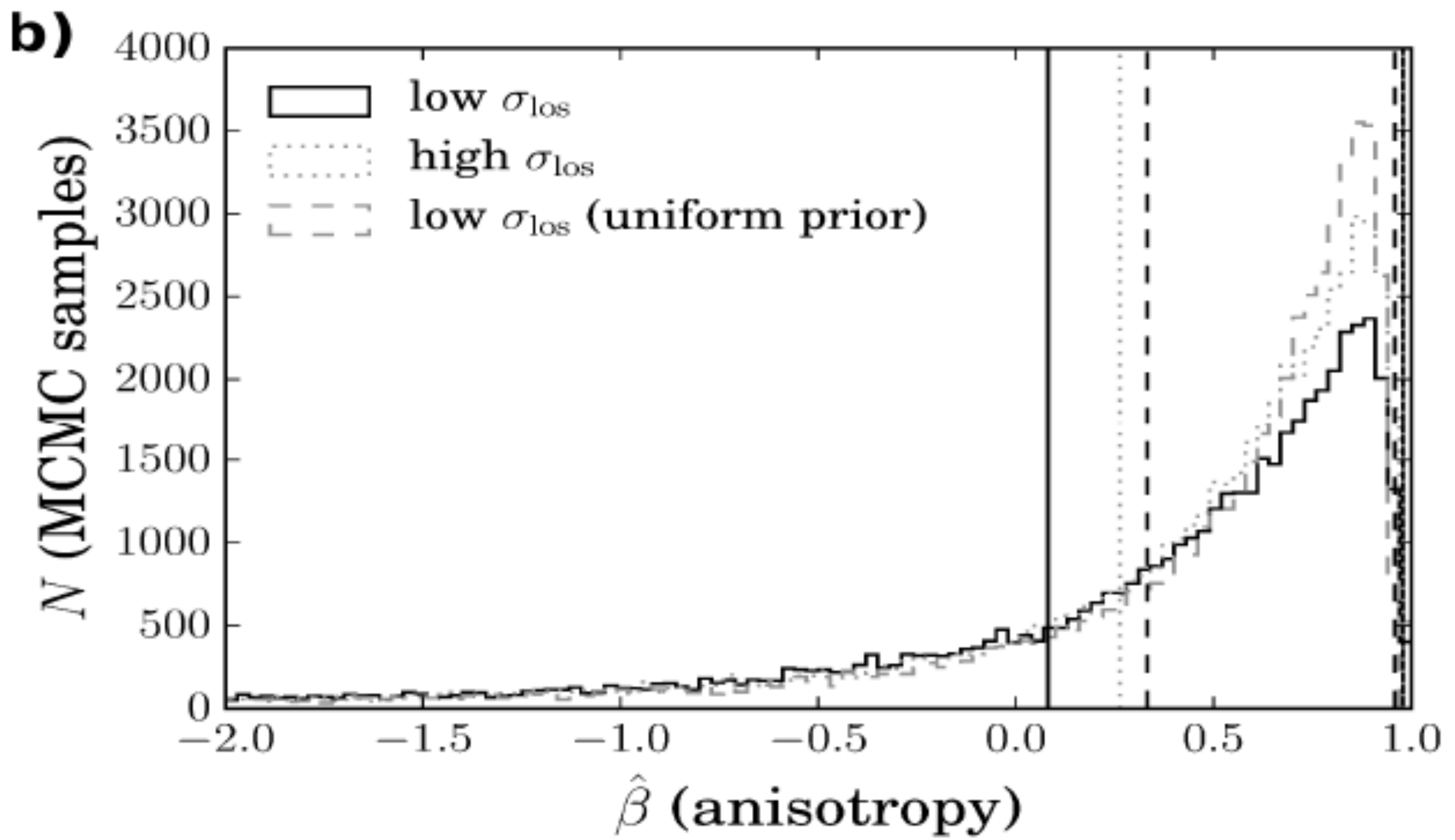

A system with a constant velocity anisotropy β as high as 0.8 is unlikely

➡ β_{ani} in Sculptor cannot be constant with radius

Binary stars

McConnachie & Cote 2010

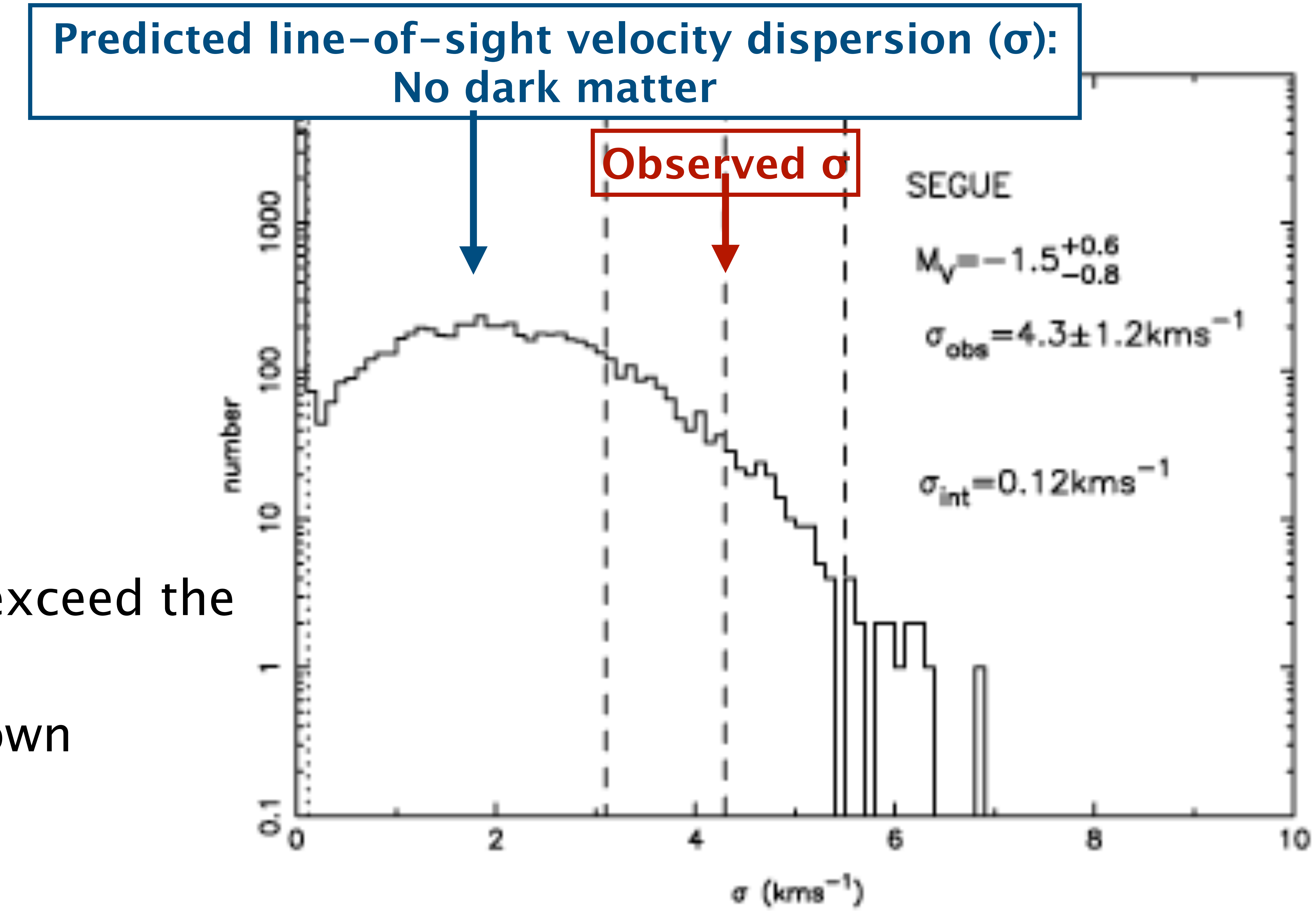

- Orbital velocities of stars in a binary system can exceed the velocity dispersion of its host dSph
- Frequency of binary stars in dSphs is not well known
  - Carina: 14^{+28}_{-5}% (Minor 2013)
  - Leo II: 30±10% (Spencer et al 2017)
    - ➡ Inflate the velocity dispersion from 2.0 km s^{-1} to 2.7 km s^{-1}
    - ➡ 80% overestimate in the galaxy's mass

Foreground contamination

* Not to scale

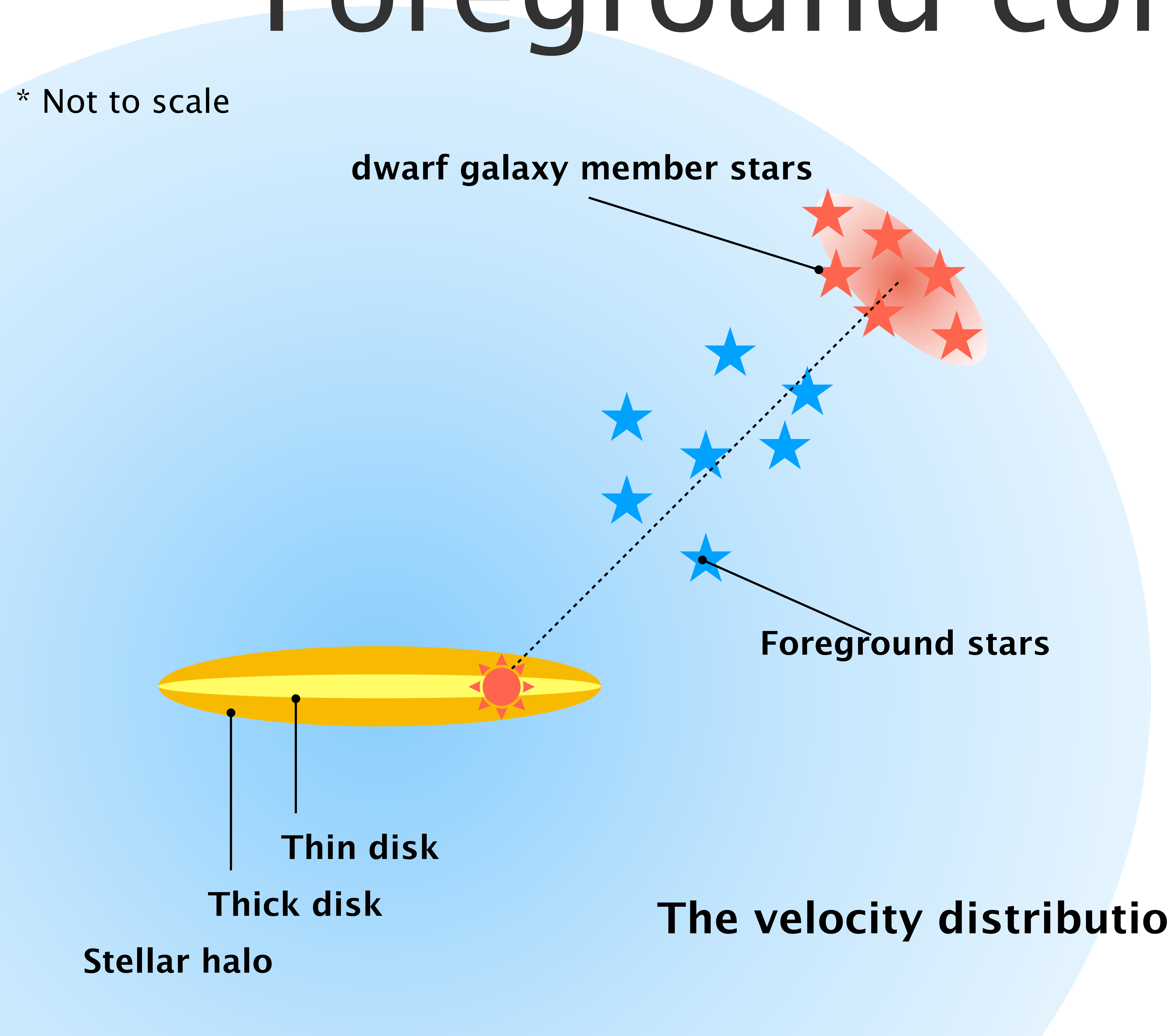

Line-of-sight velocity distribution of stars in the direction of Ursa Major I (Simon & Geha 2007)

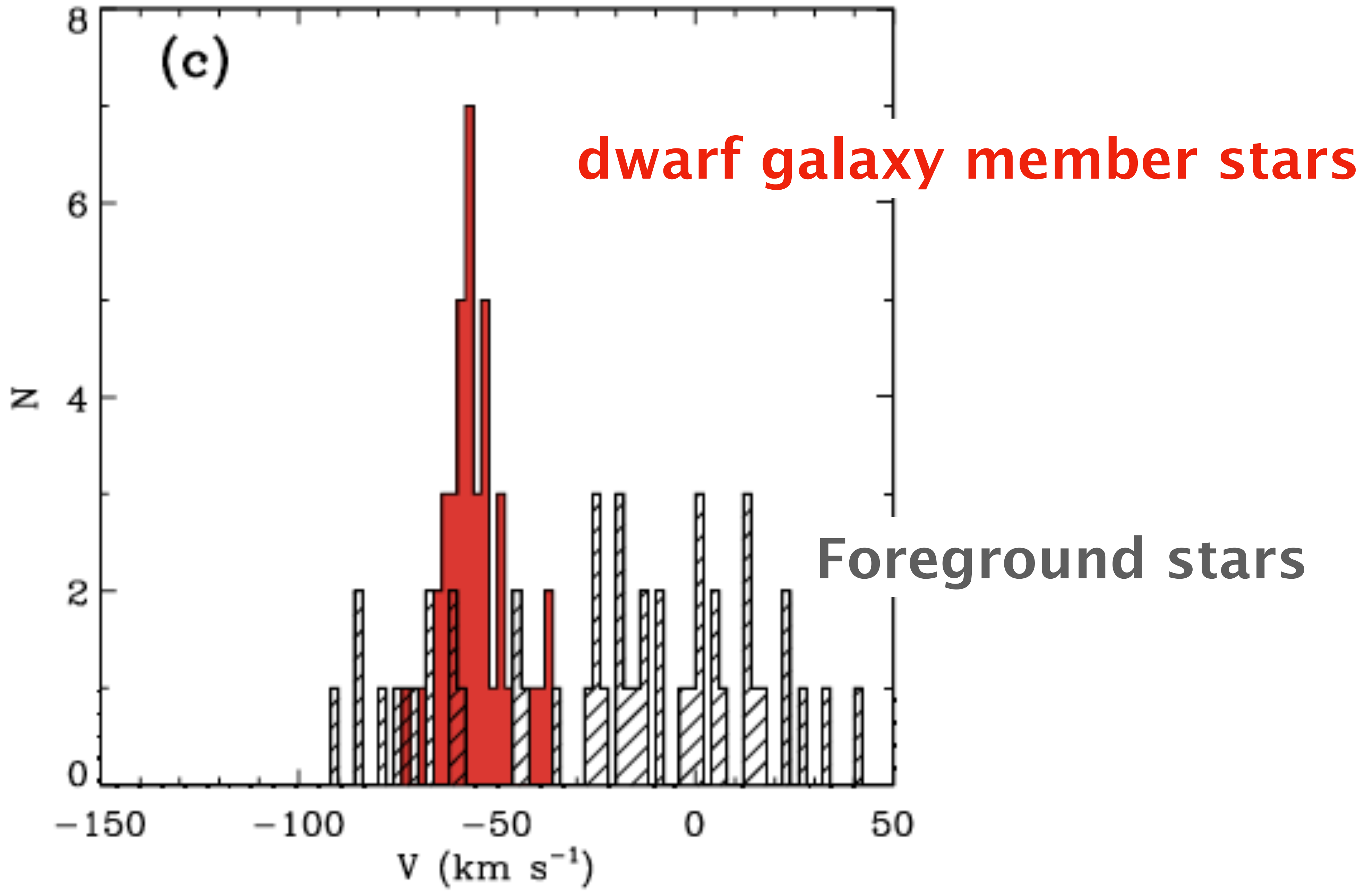

The velocity distributions overlap ➡ Contamination

The effects of FG stars in the case of Segue I

Bonnivard et al. 2016

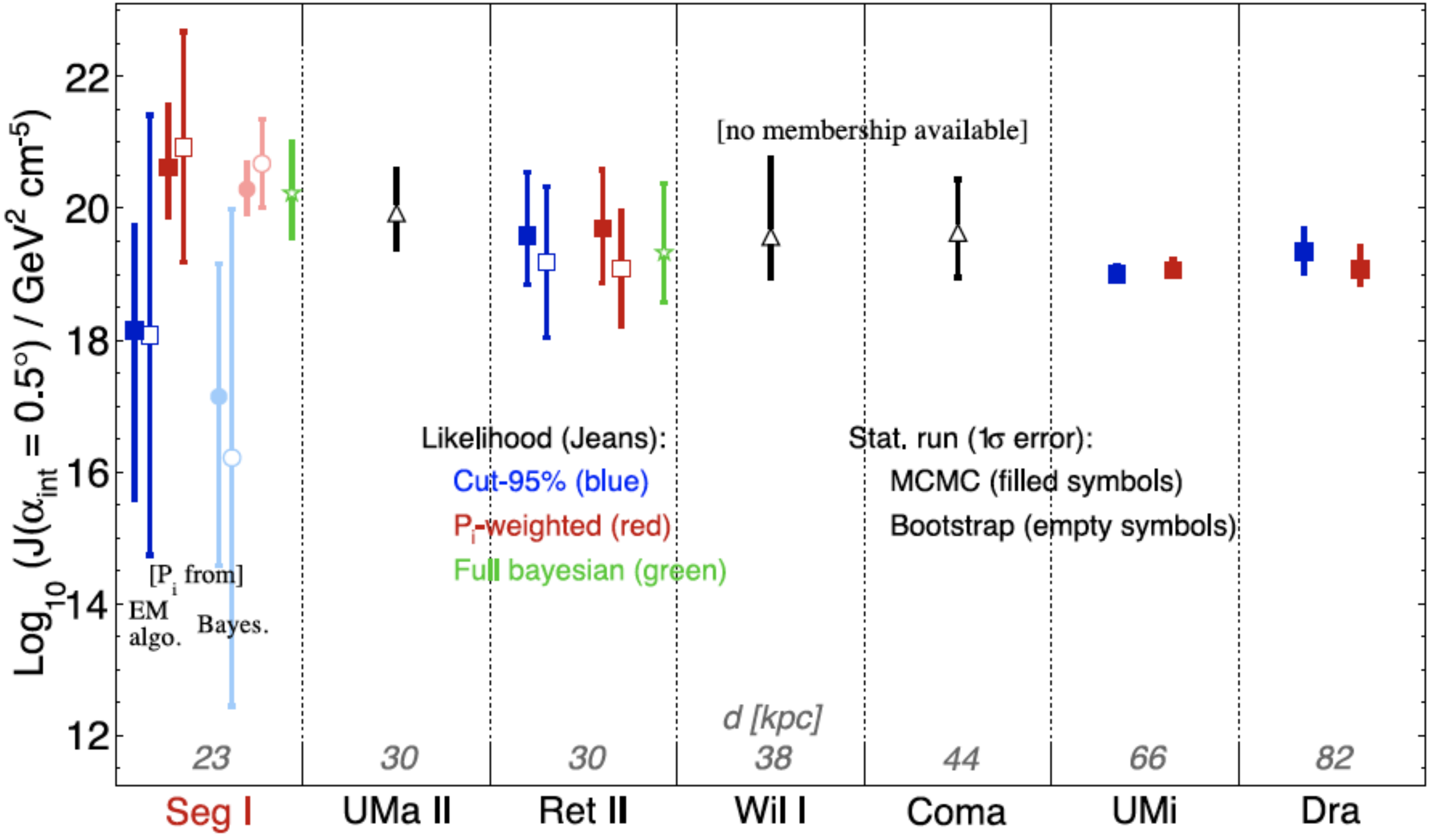

The case of Triangulum II

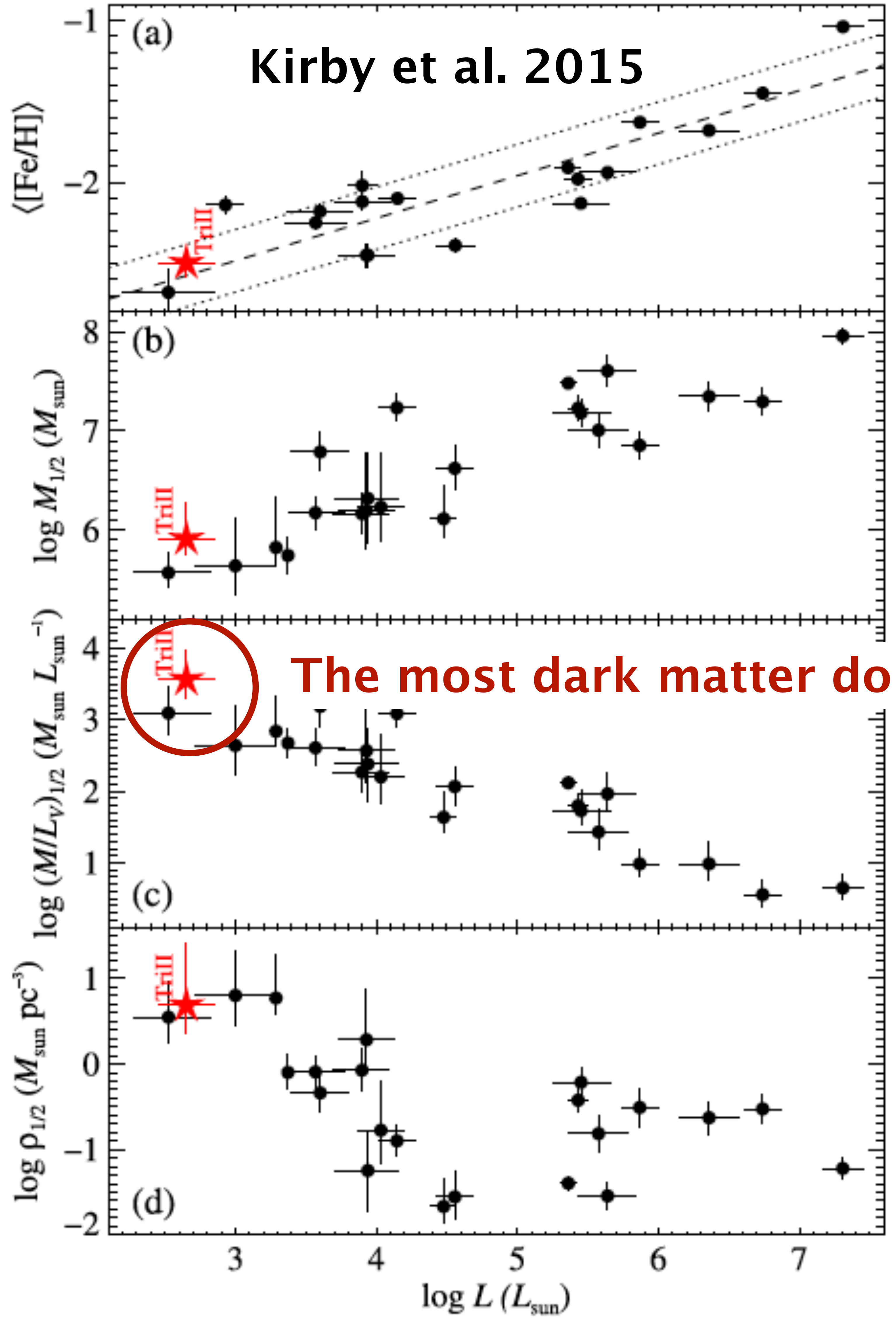

The most dark matter dominated system?

Based on 6 stars all assumed to be a single (Kirby et al. 2015)

$$\sigma_v = 5.1^{+4.0}_{-1.4}\ \mathrm{km\ s^{-1}}$$

Based on 13 stars all assumed to be a single (Martin et al. 2016)

$$\sigma_v = 4.4^{+2.8}_{-2.0}\ \mathrm{km\ s^{-1}}$$ The central 2'

$$\sigma_v = 14.1^{+5.8}_{-4.2}\ \mathrm{km\ s^{-1}}$$ The outer region

Based on 13 stars taking into account a binary (Kirby et al. 2017)

$$\sigma_v < 3.4\ \mathrm{km\ s^{-1}}\ (90\,\%\,\mathrm{C.L.})$$

Is Tri II a galaxy or a star cluster?

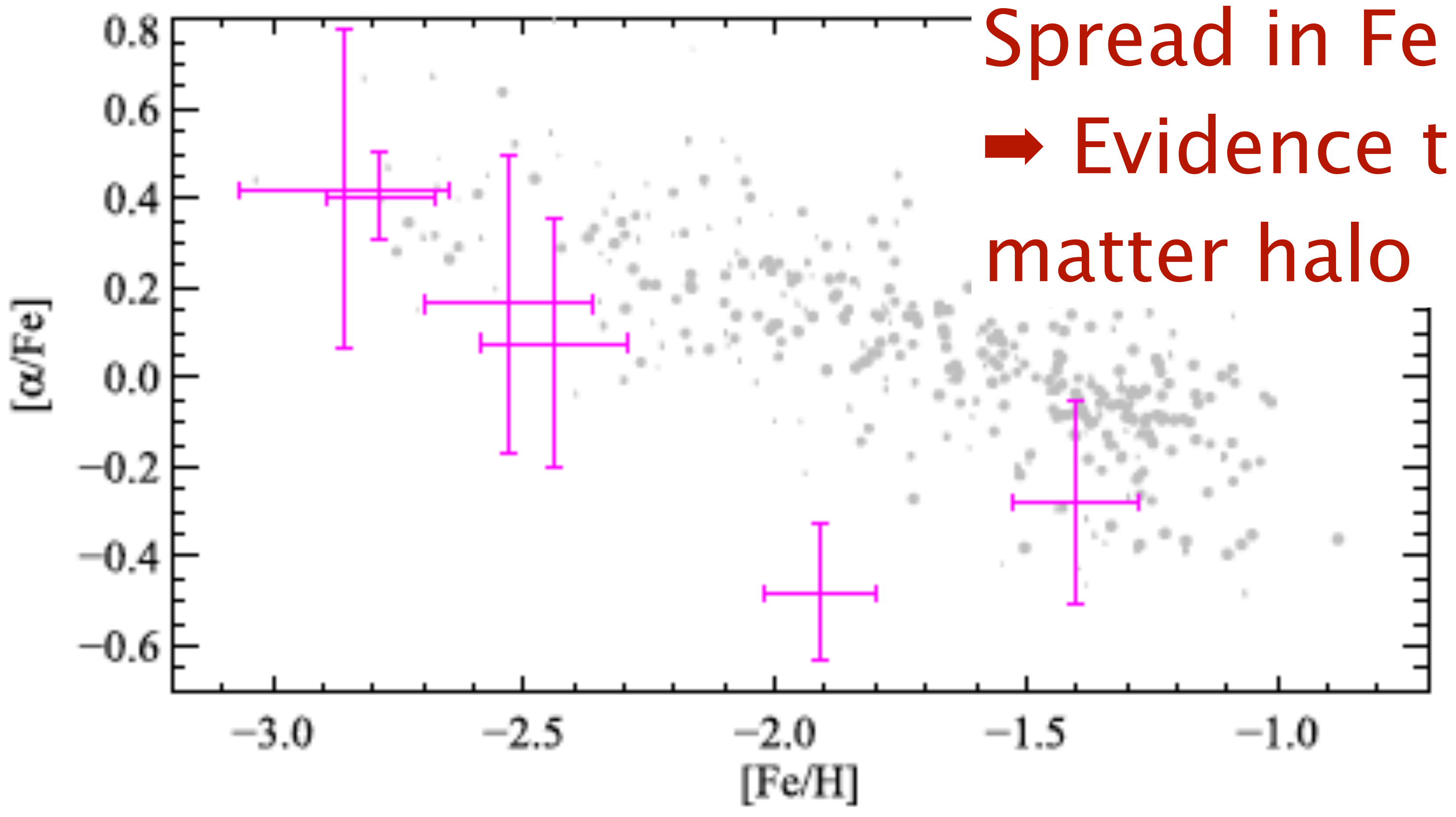

Spread in Fe and α-element (e.g. Mg, Si)
➡ Evidence that it had once embedded in dark matter halo

A set of simple cuts vs. the Expectation Maximization (EM) algorithm

① A selection box in the color-magnitude diagram

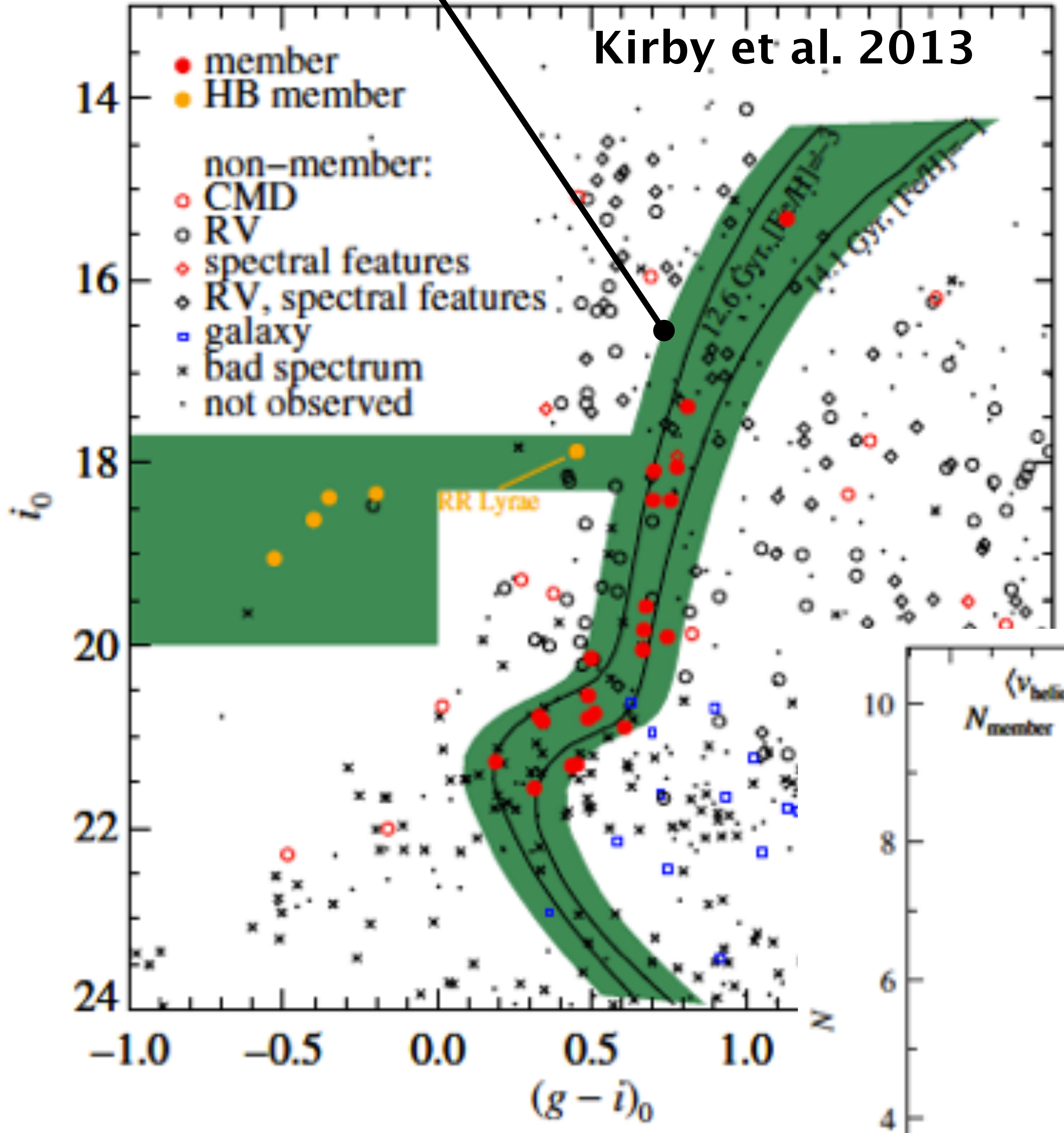

② σ clipping on V_{los}

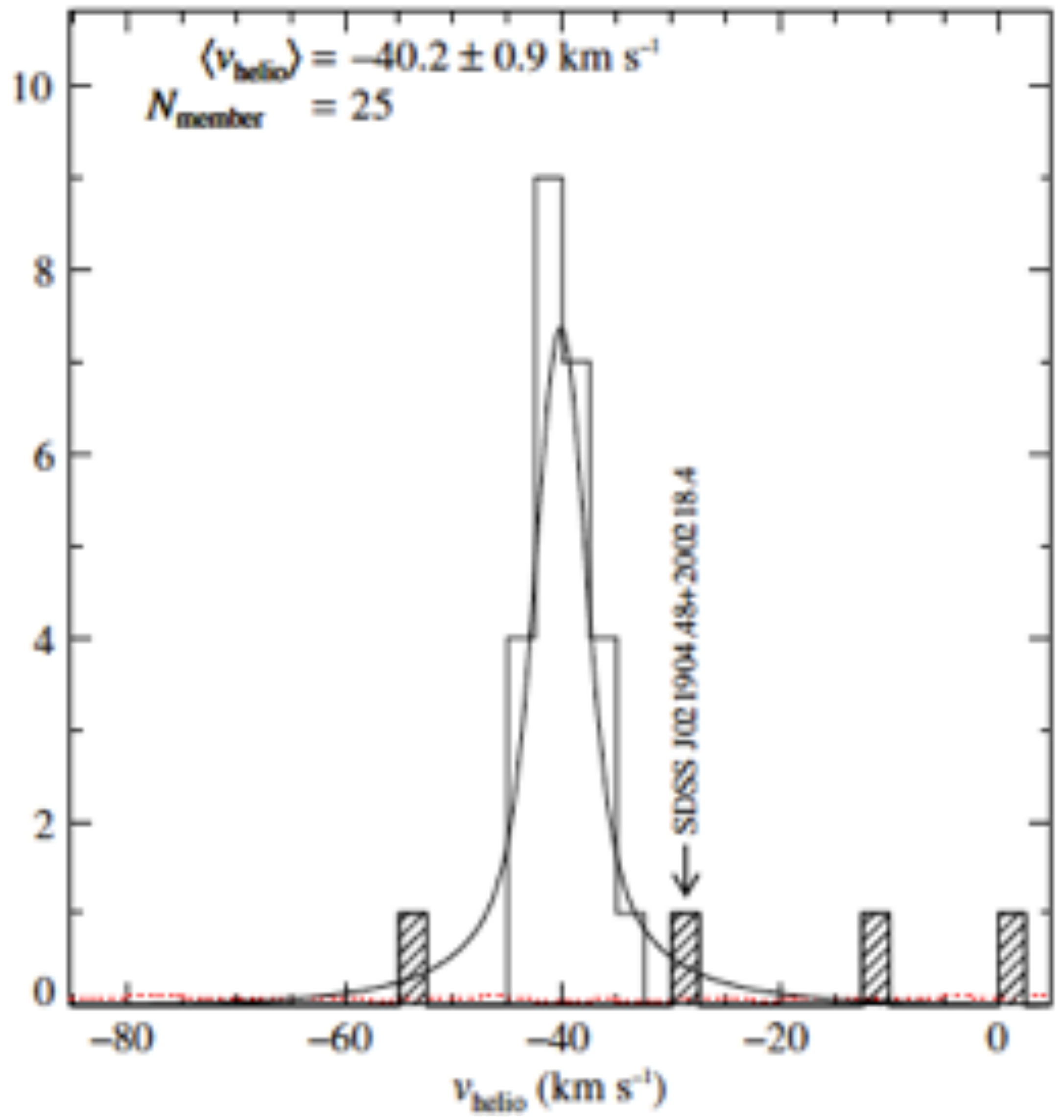

③ Surface gravity
(intrinsic luminosity)

EM algorithm calculates a probability at which a star belongs to the dSph

Walker et al. 2009

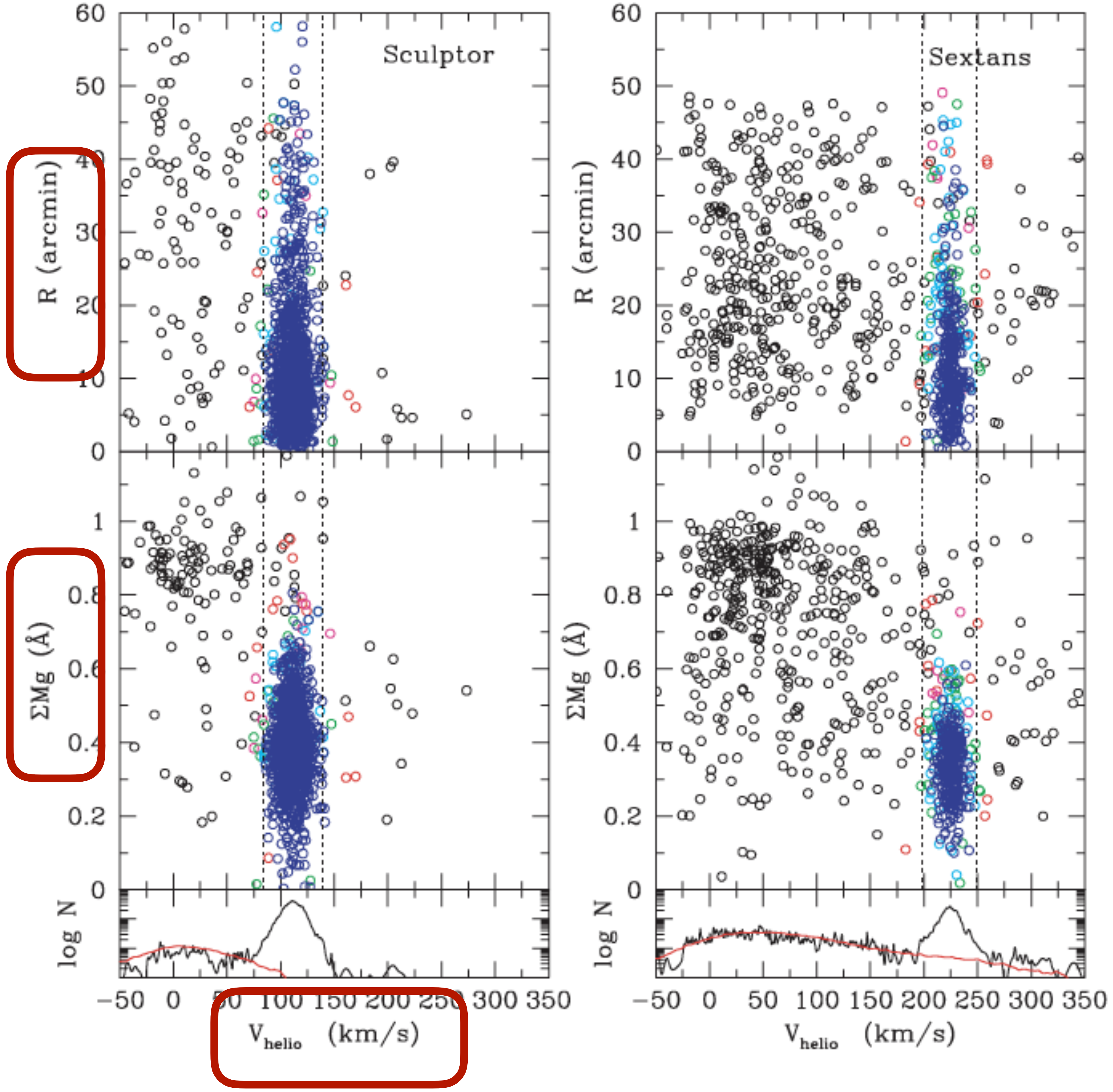

The method developed by Ichikawa+17, 18

- The likelihood function is constructed taken the FG distribution into account
- The FG distribution is modeled based on prior knowledge about the distribution of the major stellar components in the Milky Way
- After the simple cuts to exclude obvious FG contaminants, the mixed component analysis is performed
- To test the new method, we have constructed mock stellar kinematic data based on the latest observational facts about the dwarf spheroidal galaxies as well as the FG Milky Way stars

The likelihood functions

The single component fit: All stars after the simple cuts are the members

$$-2\ln L_s = -2\sum_i \ln(f_{\rm Mem}(v_i, R_i))$$

$$f_{\rm Mem}(v, R) = 2\pi R \Sigma_*(R) C_{\rm Mem} \mathcal{G}\left[v; v_{\rm Mem}, \sigma_{l.o.s.}(R)\right]$$

The mixed components fit: The stars are either a member star or a Milky Way foreground (FG) stars

$$-2\ln L_m = -2\sum_i \ln(s f_{\rm Mem}(v_i, R_i) + (1-s) f_{\rm FG}(v_i, R_i))$$

$$f_{\rm FG}(v, R) = 2\pi R C_{\rm FG} \prod_{j=1}^{3} \mathcal{G}\left[v; v_{\rm FGj}, \sigma_{\rm FGj}\right]$$

Mock classical dSphs

- Stellar color and magnitude
  - Stellar evolution model (Beressan et al. 2012)
  - Ages, chemical compositions, distances from observations
- Kinematics and position
  - Input dark matter distribution

Table 2 of Ichikawa et al. 2017

dSph	$\log_{10}(\rho_s/[M_\odot pc^{-3}])$	$\log_{10}(r_s/[pc])$	α	β	γ	$\log_{10}(1-\beta_{ani})$
Draco 1	-2.05	3.96	2.78	7.78	0.675	0.130
Draco 2	-1.52	3.15	2.77	3.18	0.783	-0.005
Ursa Minor	-0.497	2.60	1.64	5.29	0.777	-0.475

The color-magnitude diagrams for the mock data

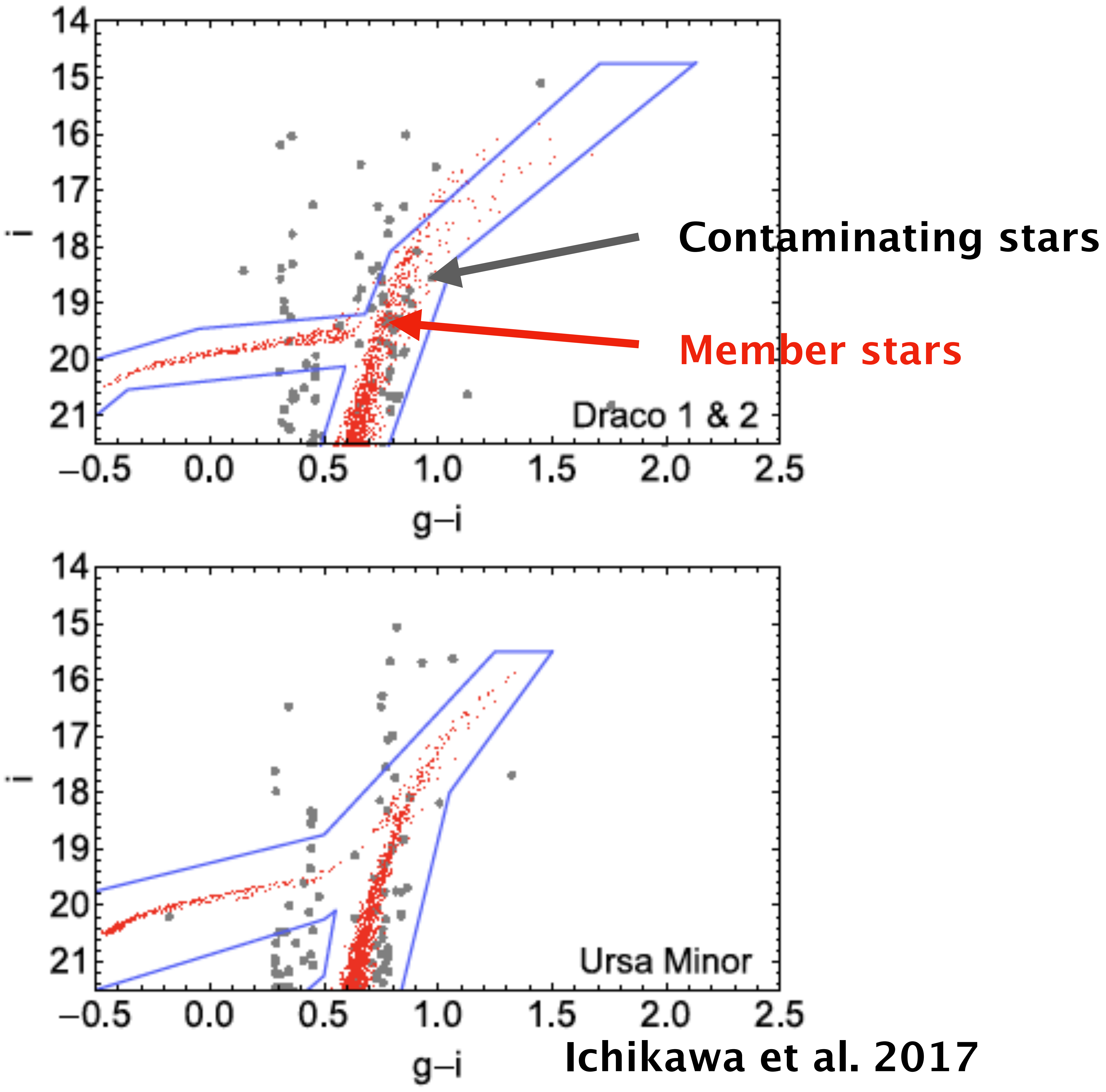

Ichikawa et al. 2017

Mock stellar data for the foreground (FG) stars

- The model stellar distribution of the Milky Way (Robin et al. 2003)
- The three major stellar components in the Milky Way
  - Thin disk
  - Thick disk
  - Stellar halo
- Simple cuts on color, apparent magnitude, surface gravity, line-of-sight velocities are applied to both the member and the FG stars

The distribution of line-of-sight velocities of FG stars in the direction of Draco

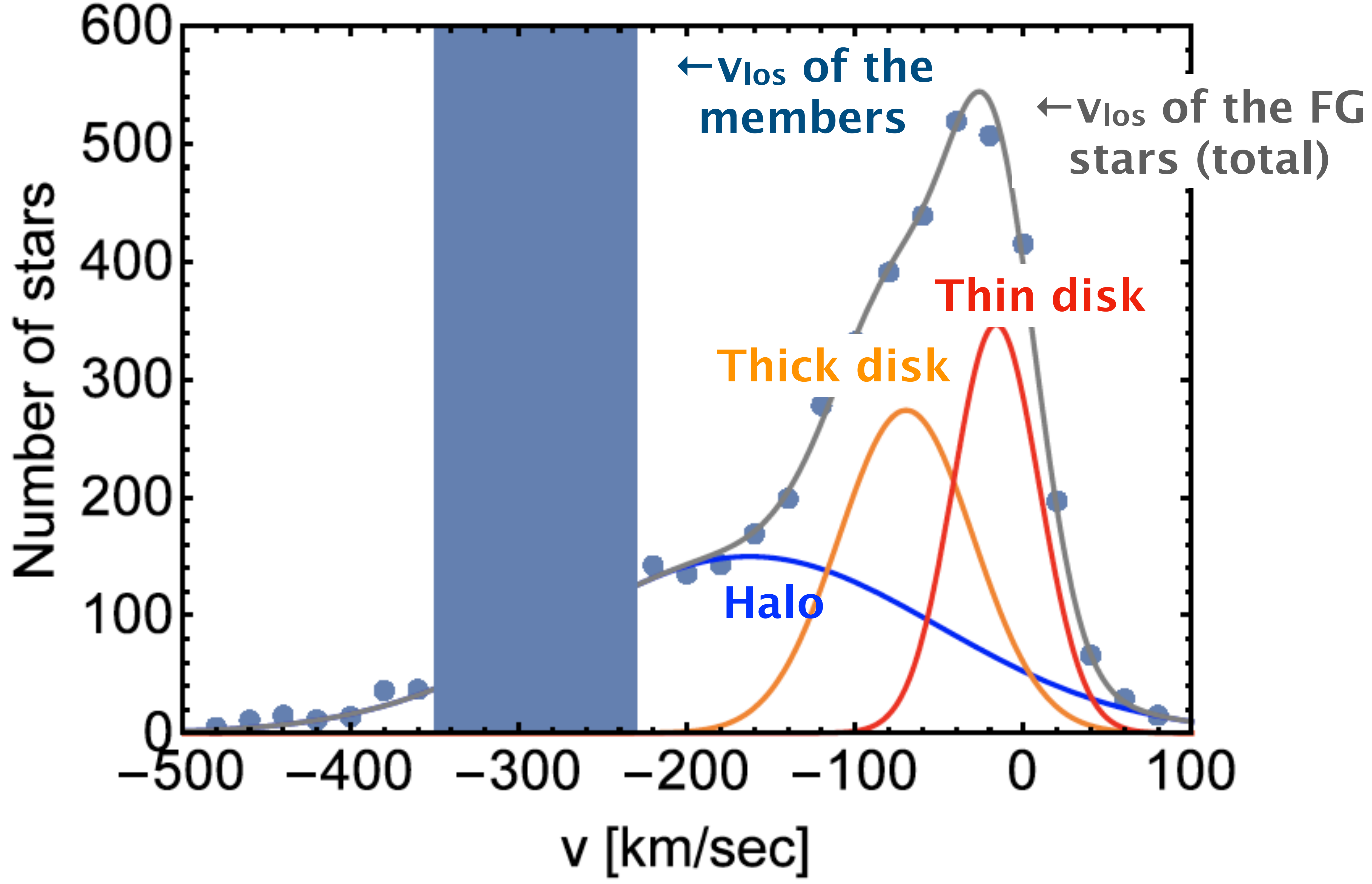

Number of contaminants after the naive cuts

Table 4 of Ichikawa et al. 2017

	Field of view (radius°)	Limiting magnitude in i-band	N_{mem}	N_{FG}	
Draco	Small (0.65)	19.5	260	16	Conventional limit
		21.0	900	37	Future conservative limit
		21.5	1140	43	Future optimistic limit
	Large (1.3)	21	940	150	
Ursa Minor	Small (0.65)	19.5	290	10	Conventional limit
		21.0	1100	33	Future conservative limit
		21.5	1400	41	Future optimistic limit
	Large (1.3)	21.0	1130	140	

- Small field of view: ~ 3–6% contaminants
- Large field of view: up to 16% contaminants
- Relative fraction of contaminants decrease with deeper observations

The single vs mixed component fit

J-factors based on 50 mock data for each of the Draco1, Draco2 and Ursa Minor

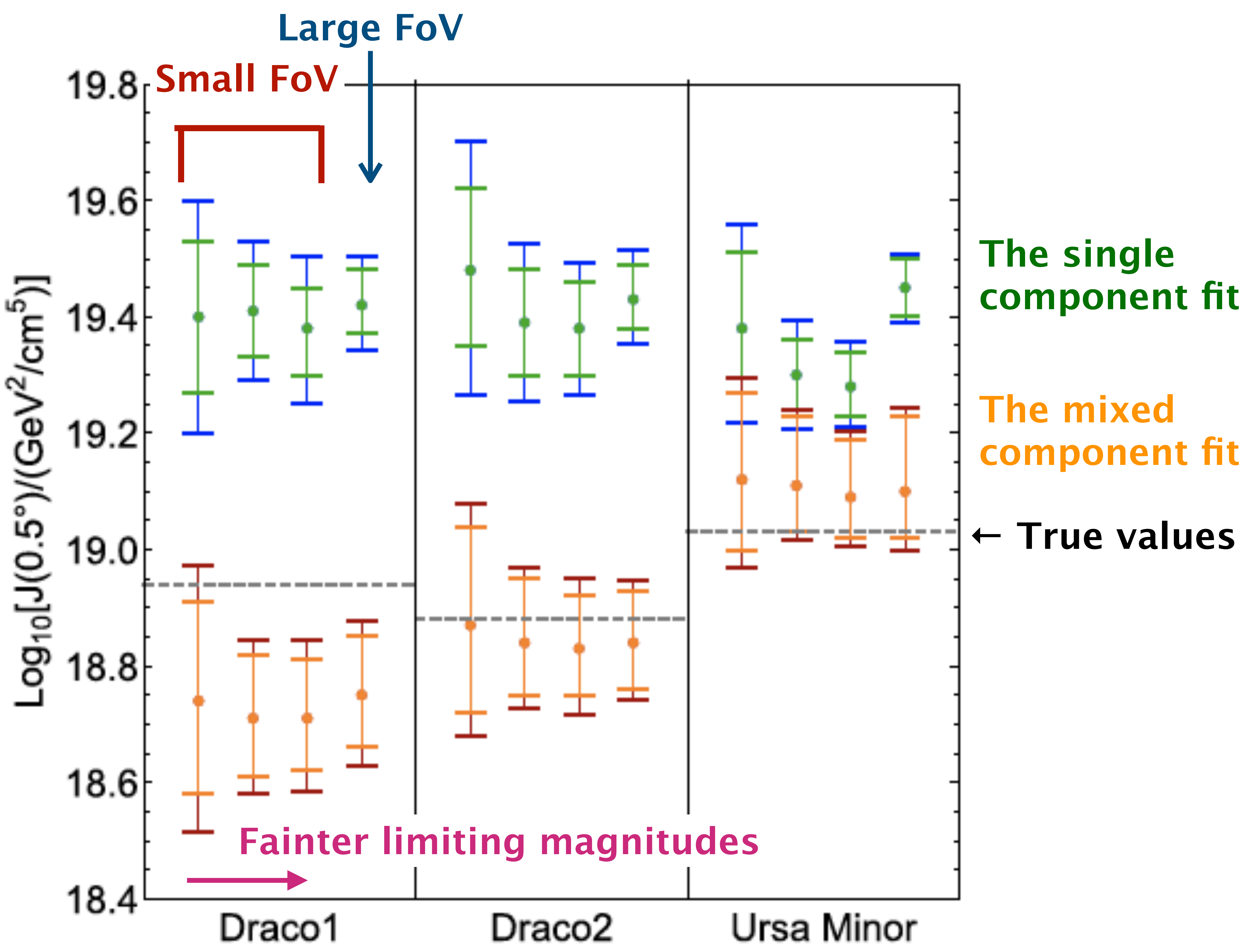

Ichikawa et al. 2017

- The 3-6% FG contaminantion can overestimate the J-factor up to a factor of ~3 (the single component fit)
- The mixed component fits result in smaller bias
- Reduction of the errors by 20-30% by deeper (fainter) observations
- The single component fit would return a biased result by wider field of view

Velocity dispersion profile

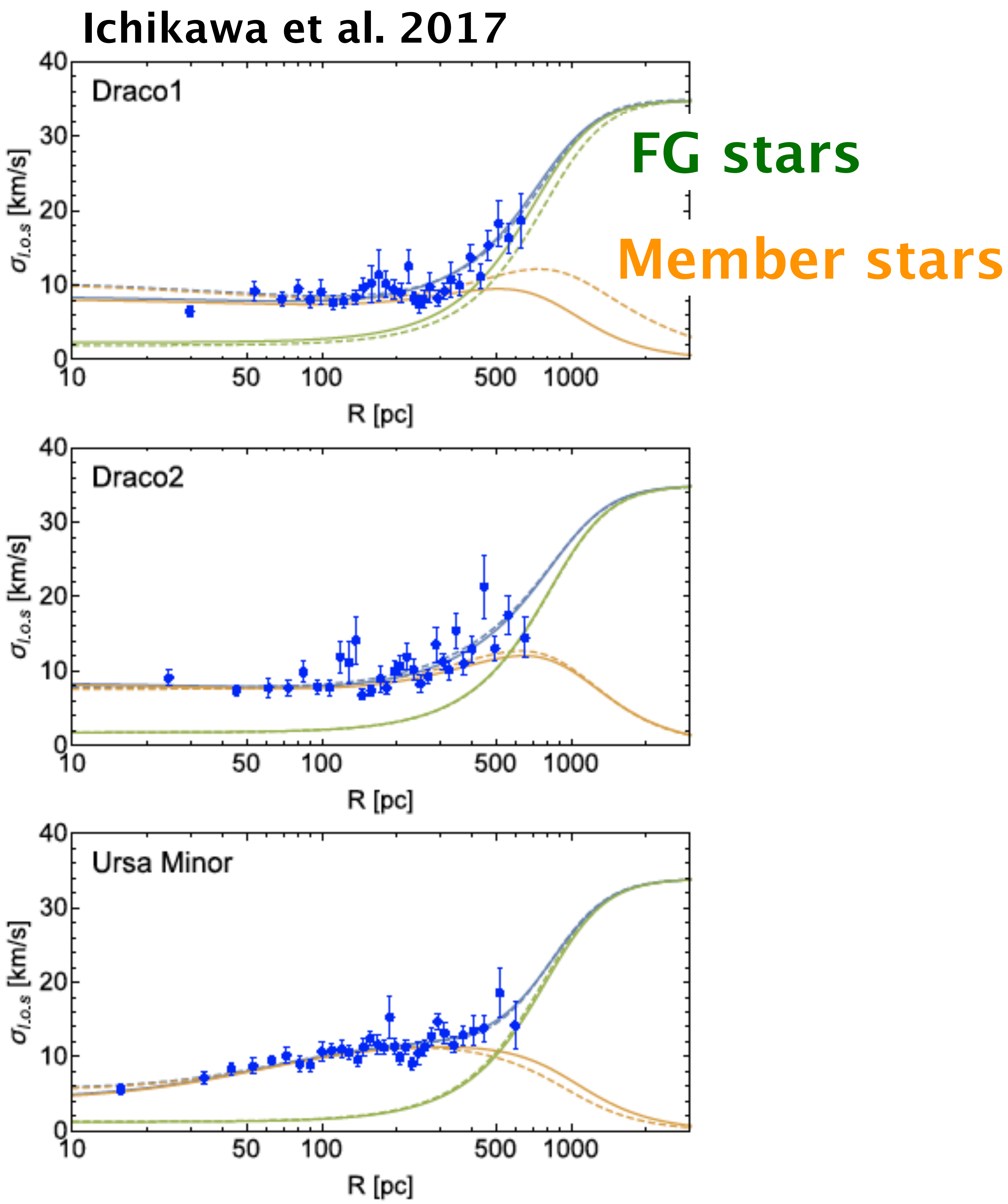

- The effect of FG stars become significant at regions outside the half-light radius (~ 200 pc)
- If the FG stars in the outer regions are erroneously treated as the member stars, the results will be biased
- The effect of the FG contamination would not be reflected to the errors
- More important for future wide-field dSph surveys

Comparison with the EM algorithm

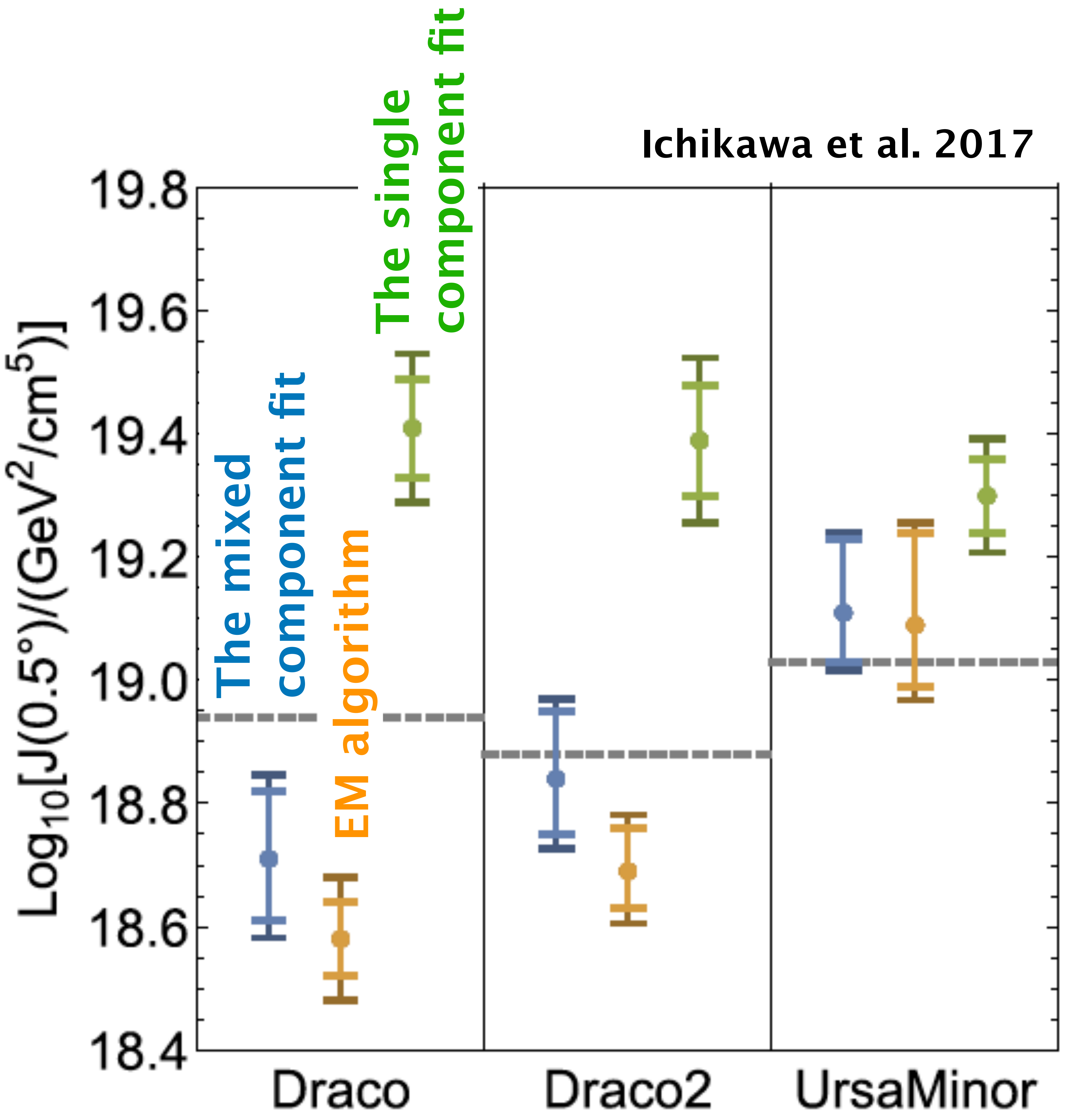

- The EM fit better reproduces the input value than the single component fit

- The mixed component fit better reproduce the input for the case of Draco-like dSph

The EM algorithm employs a prior assumption of the velocity dispersion profile of the dSph

➡ Biased result if the assumption is not valid

Mock ultra-faint dwarf galaxies

Ichikawa, Horigome et al. 2018

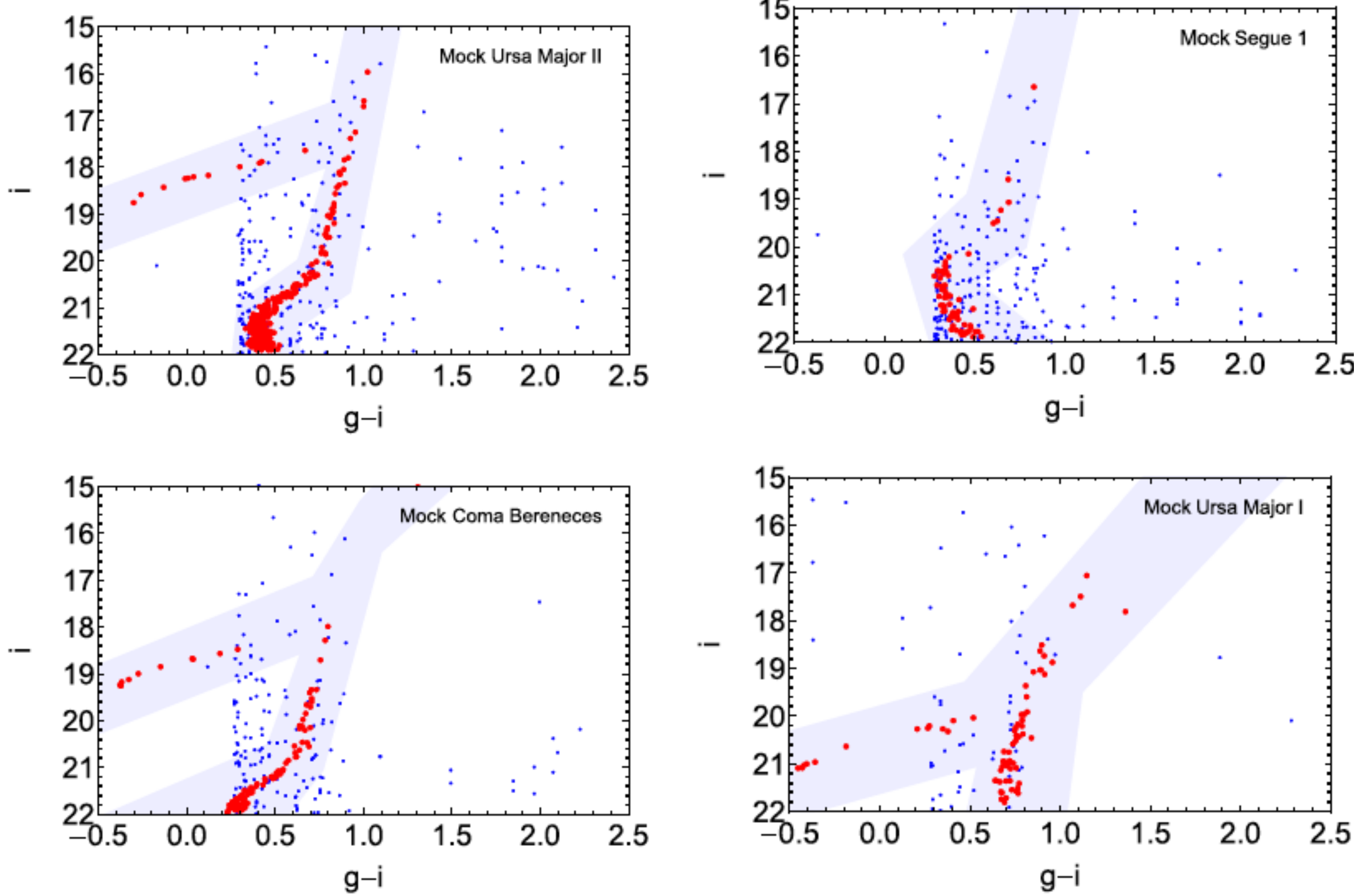

Expected contaminants

The FG contamination can be larger than the member stars

The EM method can efficiently exclude the FG

Table 3 of Ichikawa, Horigome et al. 2018

	Condition		Raw		Naive cut		Membership selection	
Model dSph	θ_{ROI} (deg)	$i_{\max}$ (mag)	N_{Mem}	N_{FG}	N_{Mem}	N_{FG}	N_{Mem}	N_{FG}
Ursa Major II	0.65	21	80	829	76	75	54	5
		21.5	150	988	141	103	89	4
		22	233	1149	214	132	131	4
Coma Berenices	0.65	21	35	579	34	58	29	2
		21.5	58	743	55	85	44	2
		22	92	898	85	110	66	1
Segue 1	0.65	21	24	620	22	60	19	1
		21.5	43	748	39	84	34	0
		22	61	953	56	123	49	0
Ursa Major I	0.65	21	42	680	37	32	26	1
		21.5	55	831	48	39	34	1
		22	63	953	56	44	38	1

J–factor estimates

Ichikawa, Horigome et al. 2018

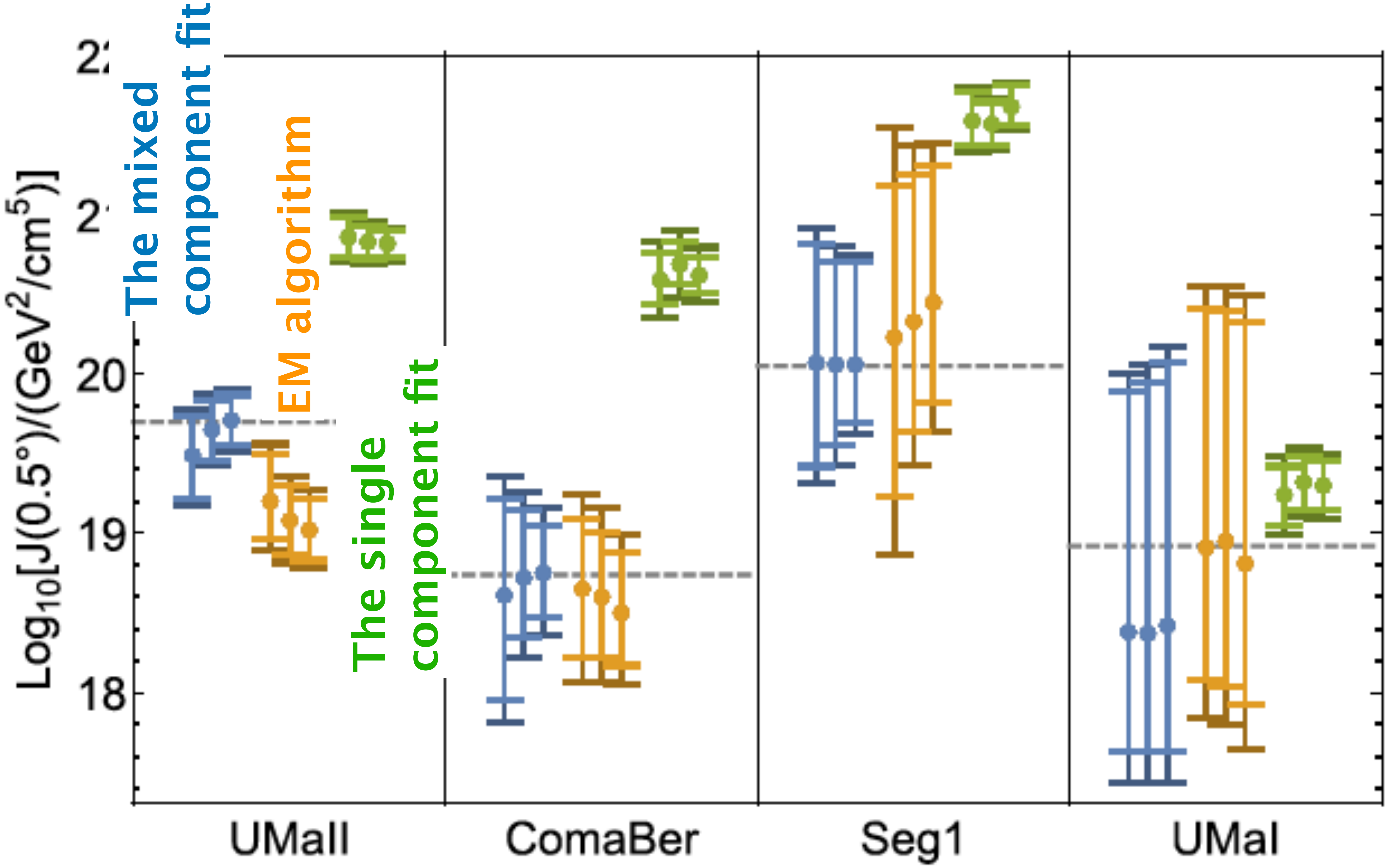

Fainter limiting magnitudes →

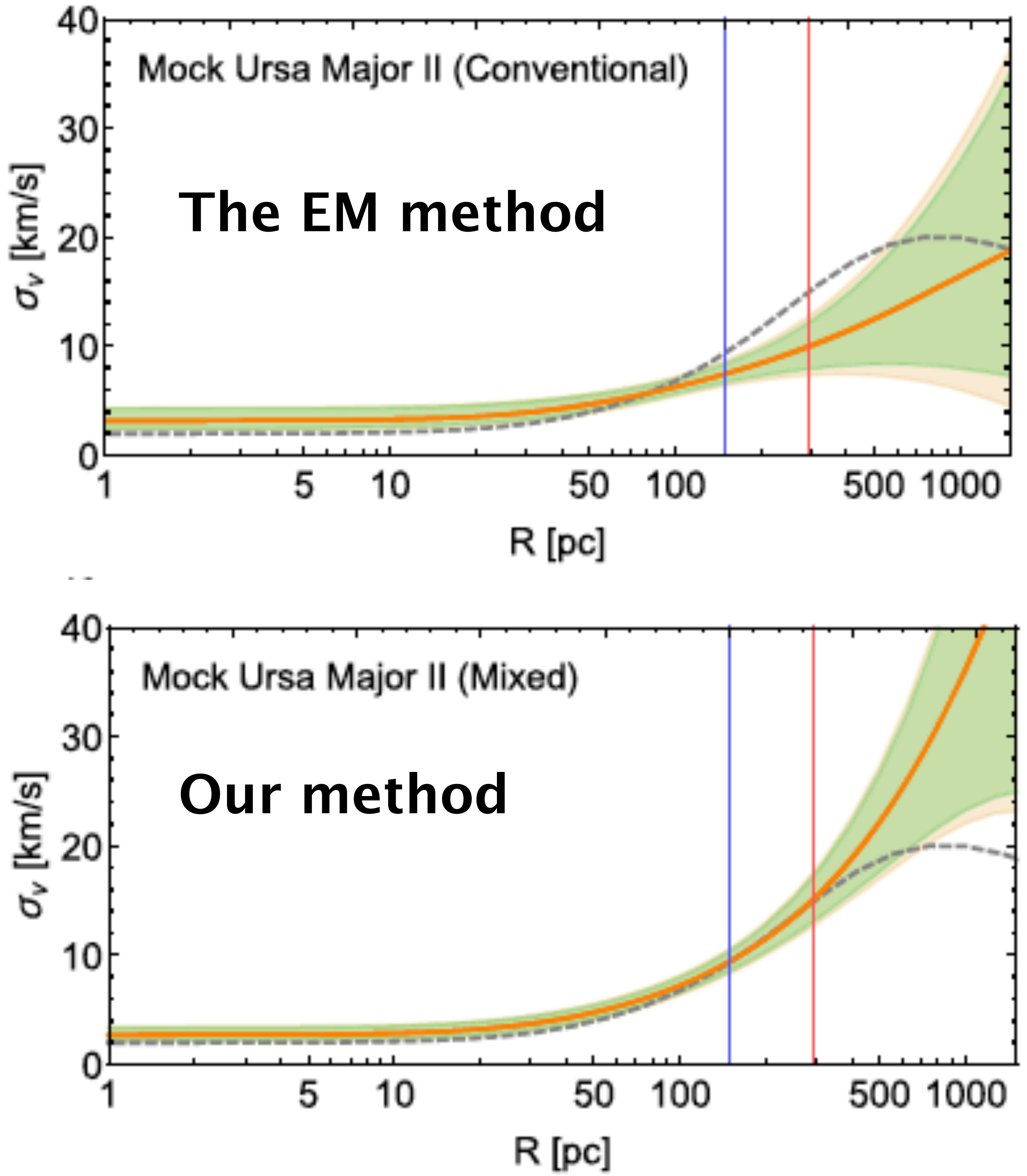

Application to the real data is ongoing

Horigome et al. in prep

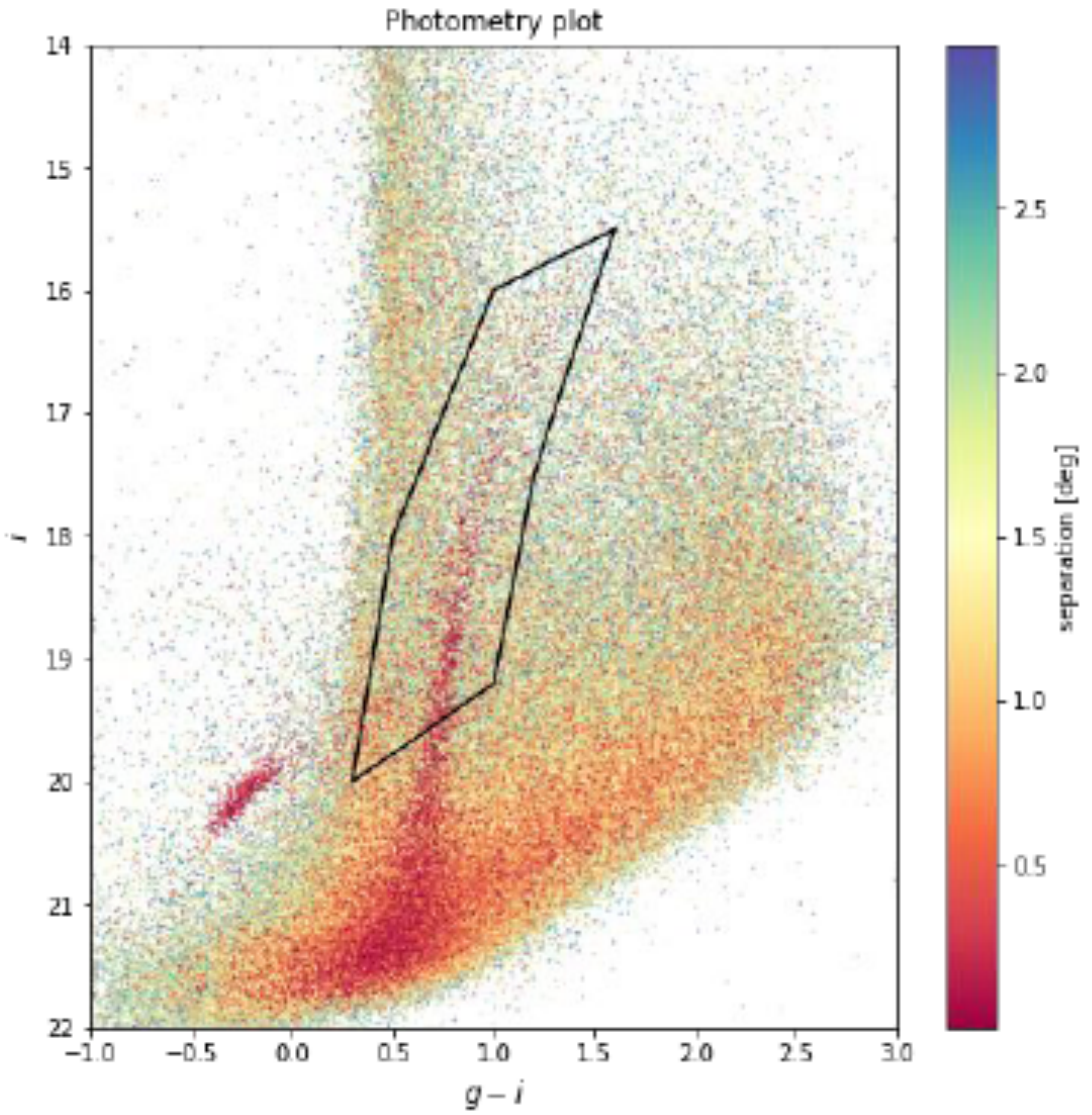

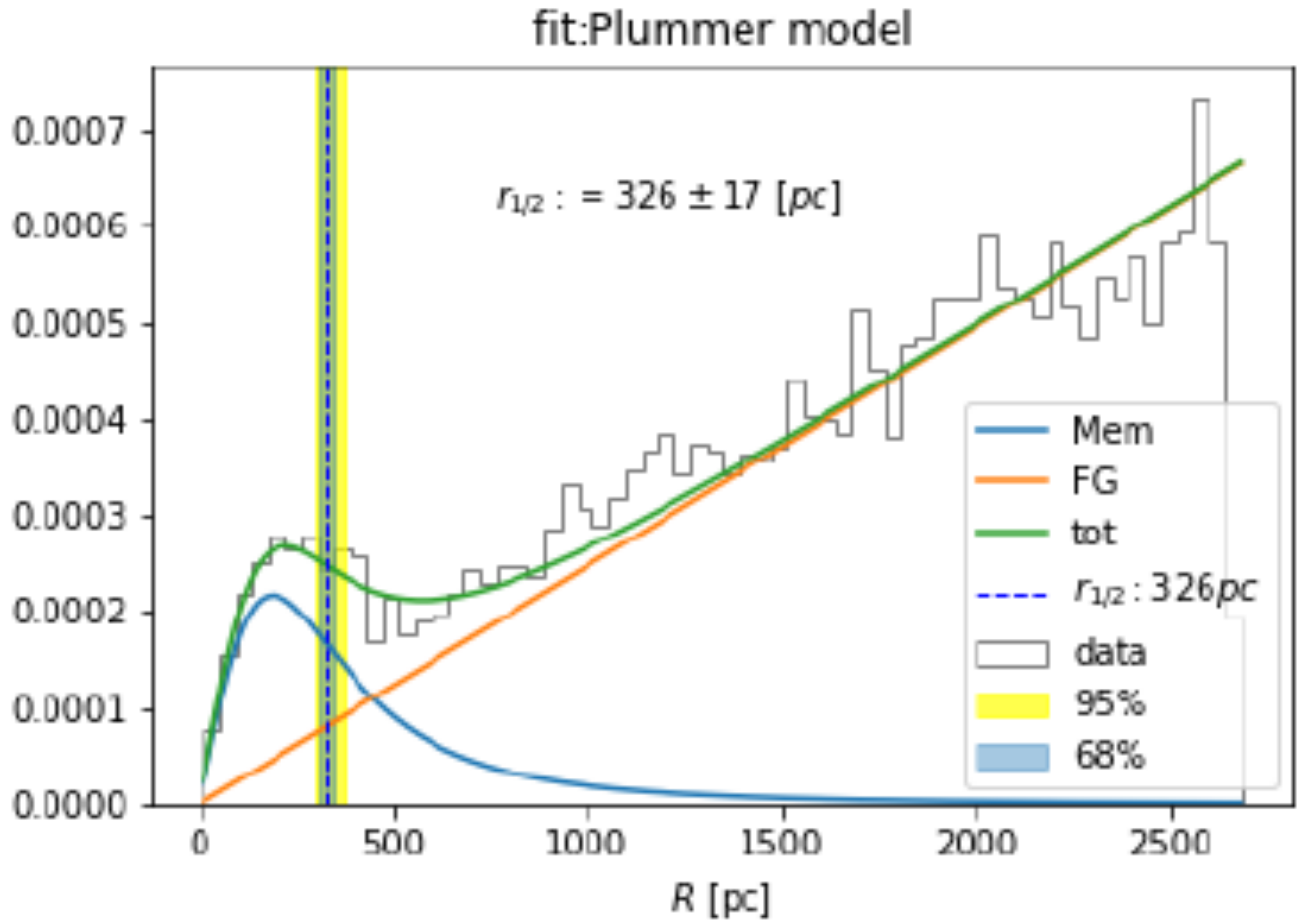

Detailed verification of prior dependence, parameter correlations, dependence on FG distributions
➡ Optimization of the future observation

Stellar kinematic measurements for dSphs in the future

- Near future
  - More than a factor of 3-5 increase in the sample size for the line-of-sight velocity measurements with new multi-object spectrographs e.g. Subaru/PFS
  - Multi-epoch spectroscopy to evaluate the binary star contamination
  - Chemodynamical analysis
  - Better constraints on the orbital motion of dSphs around the Milky Way
- Far future
  - Tangential velocity of individual stars in dSphs from precise proper motion measurements

Wide and deep dSph surveys with Subaru/PFS

Spectrographs

Red: 630-970nm (LR),710-885nm (MR)

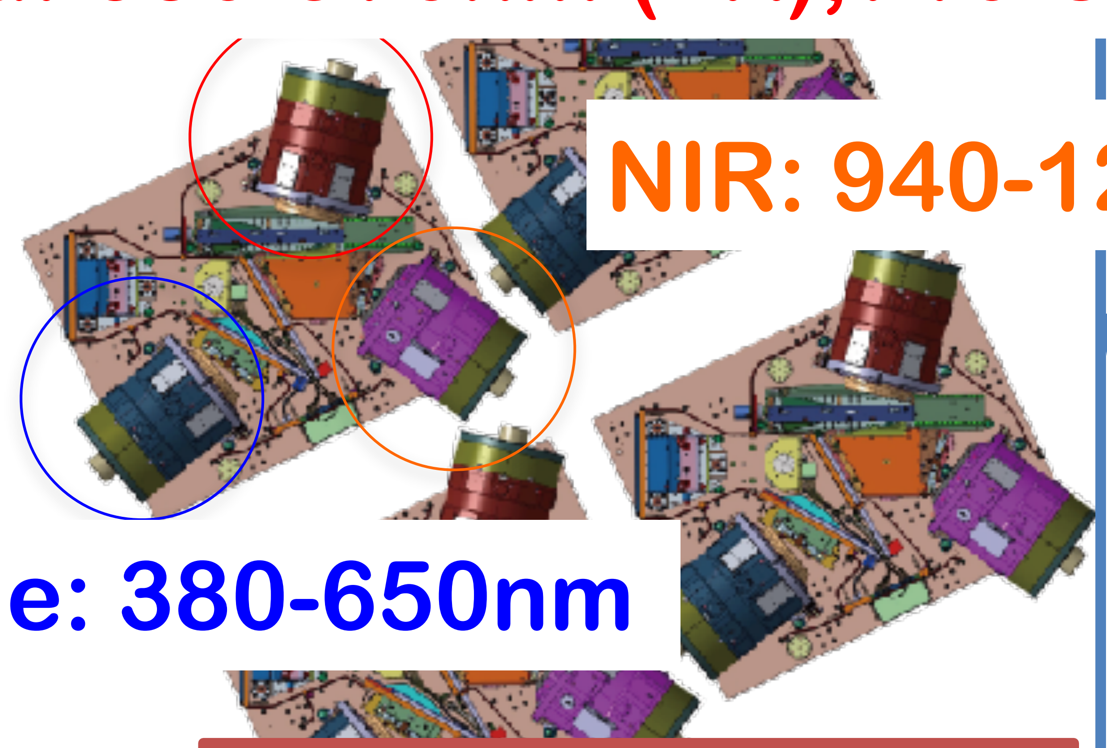

NIR: 940-1260nm

Blue: 380-650nm

LR: R~2000-4000
MR: R~5000

Metrology camera

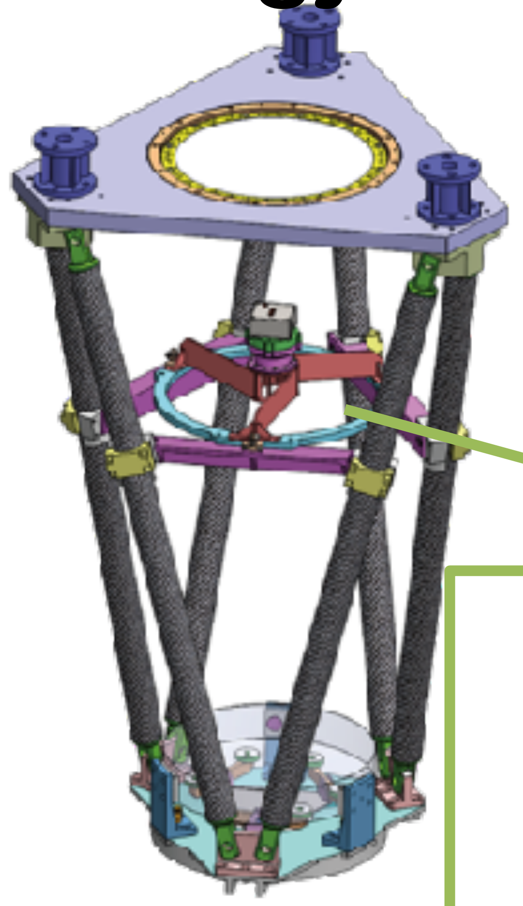

Accurate and quick fiber allocation

Subaru Telescope

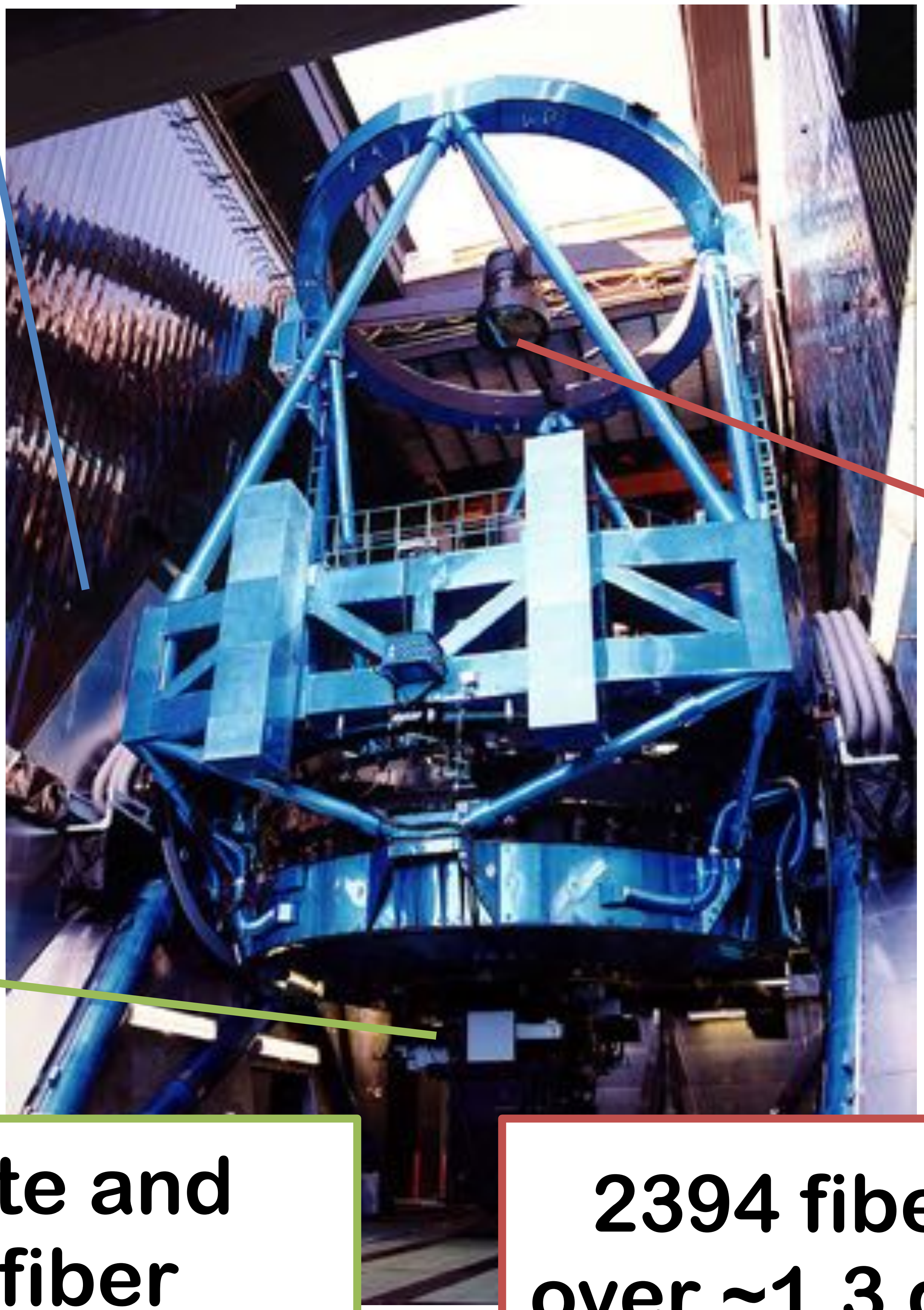

Wide-field corrector

Prime Focus Instrument

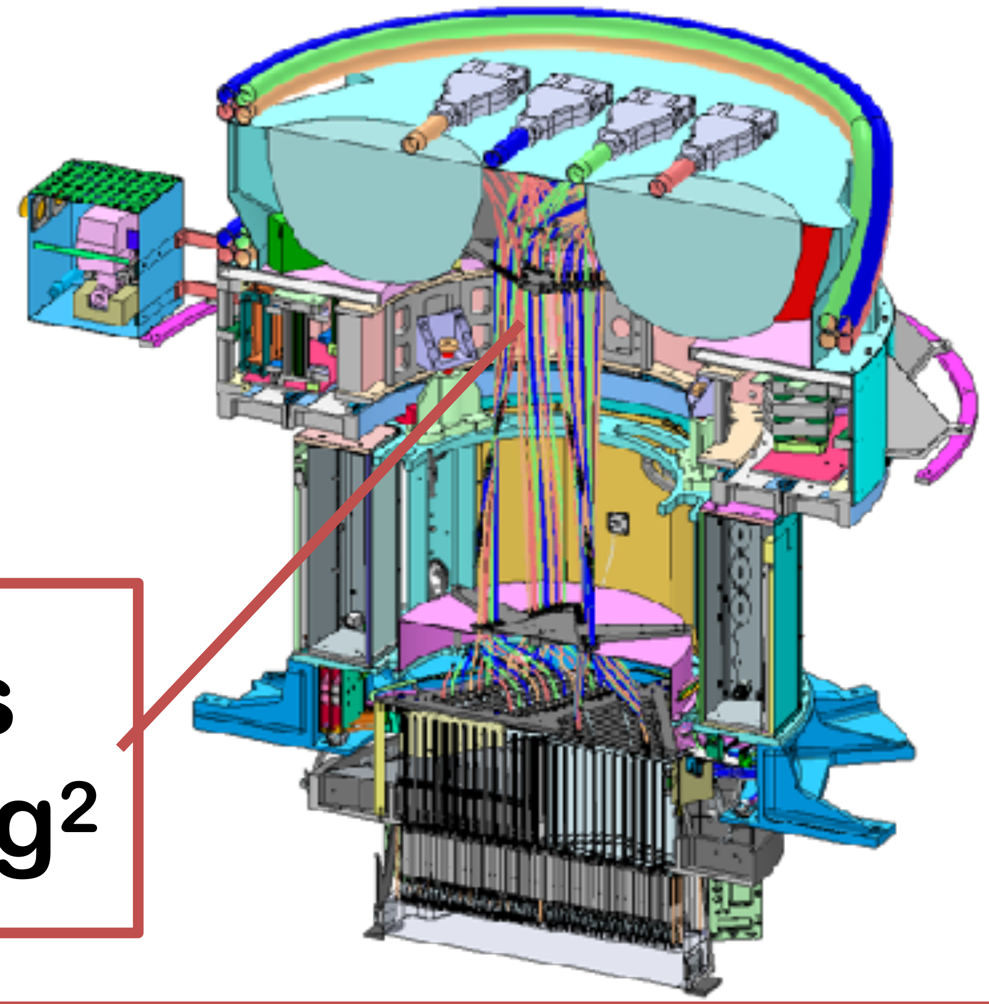

2394 fibers over ~1.3 deg^2

Field-of-view comparison

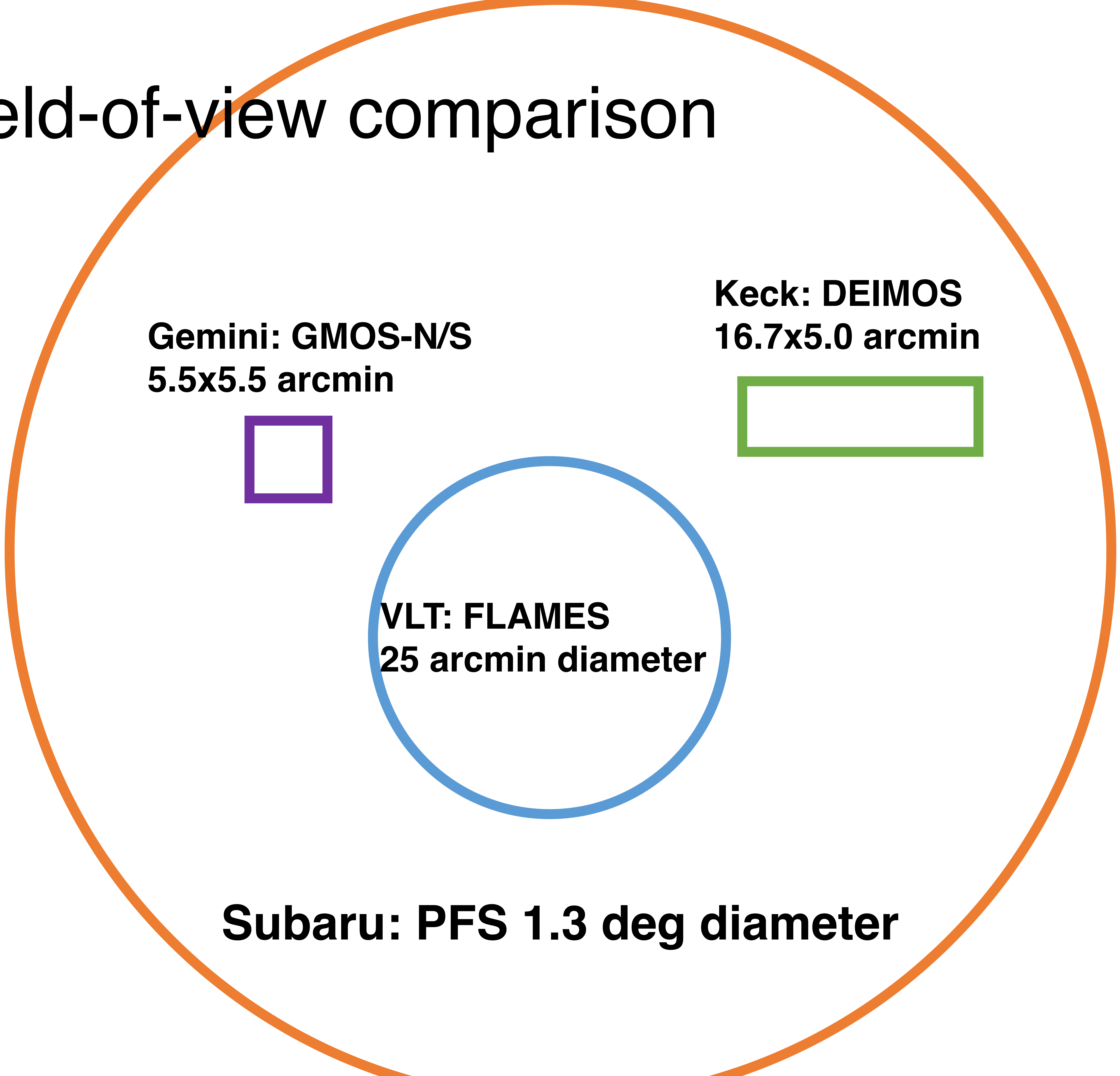

The widest FoV among optical multi-object spectrographs installed at 8-10m-class telescopes

FG contamination is more important in future observations

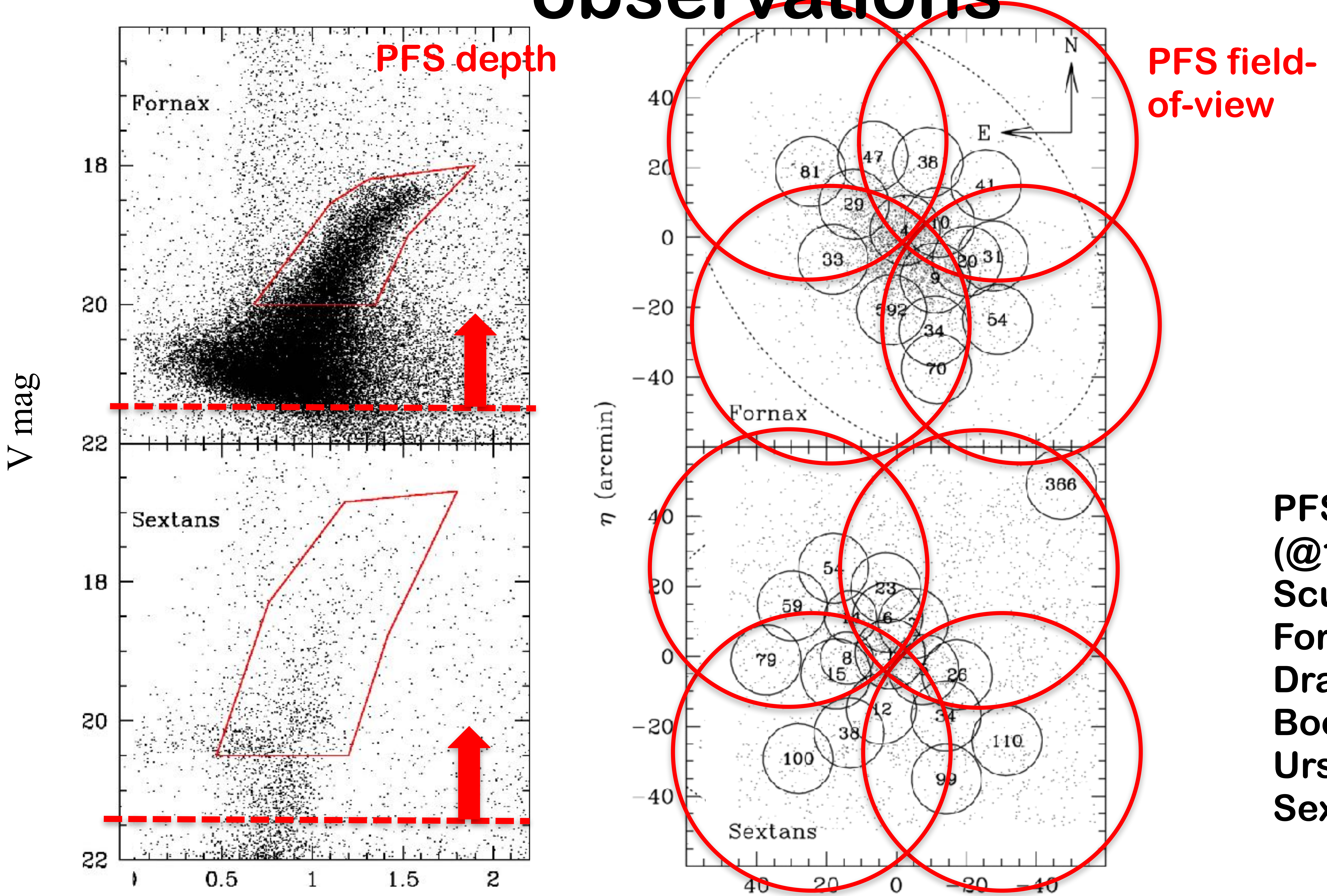

PFS-GA-plan (@12/2018):
Sculptor
Fornax
Draco
BootesI
Ursa Minor
Sextans

Walker et al. 2009, AJ, 137, 3100; Walker et al. 2009, ApJS, 171, 389

Chemodynamical analysis is the key for the core/cusp DM profiles in dSphs

Walker & Penarubia 2011

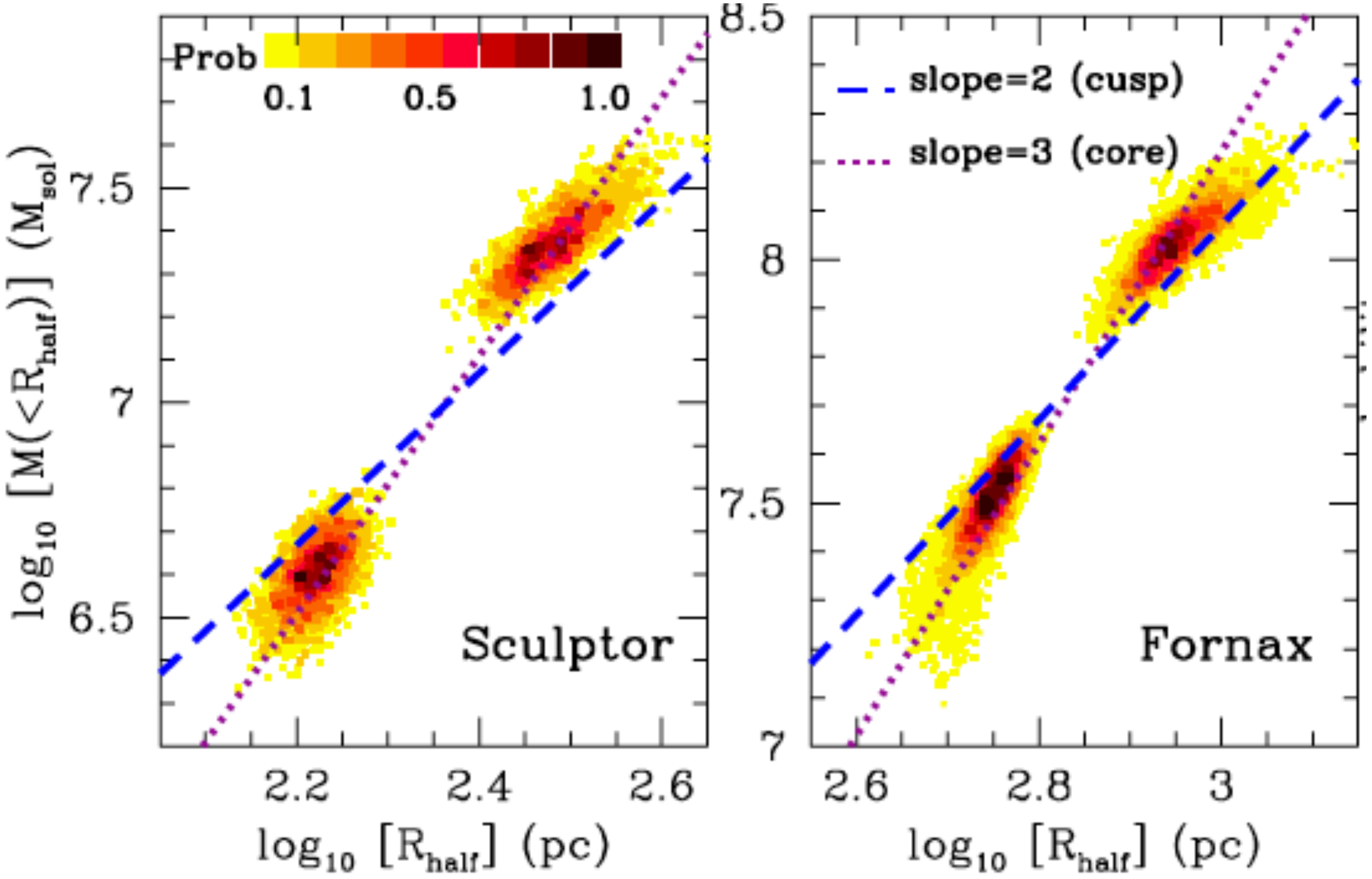

Prepared by Hayashi & Chiba

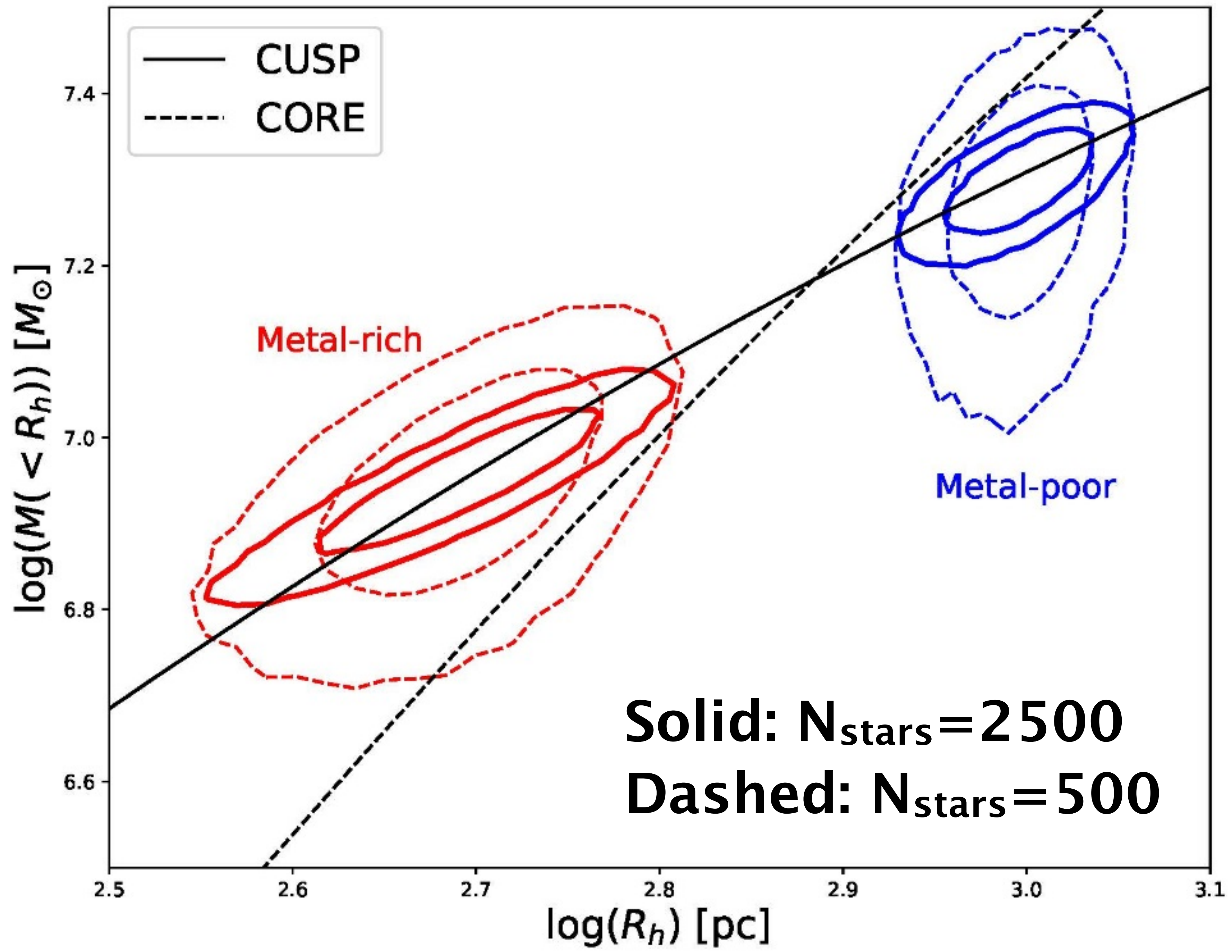

Mass enclosed by half-light radius evaluated by the two chemo-dynamically different subcomponents

➡ Dark matter density slope

Summary

- Estimates of dark matter profile in dwarf galaxies based on stellar kinematic measurements can suffer from various astrophysical uncertainties

- We have quantified the uncertainty in J-factor due to the contamination in stellar kinematic samples by constructing realistic mock stellar samples for classical and ultra-faint dwarf galaxies

- For the dSphs studied in Ichikawa+17, 18,

  - Only 3-6% FG contamination leads to biased J-factor estimation by a factor of ~ 3

  - The analysis based on the new likelihood better recovers the input parameters than the EM algorithm

- The method developed by this study will be powerful with larger samples obtained by future spectroscopic facilities